Isotope tracers of core formation

BERNARD BOURDON[1], MATHIEU ROSKOSZ[2] AND REMCO C. HIN[3]

[1] Laboratoire de Géologie de Lyon, ENS de Lyon, UCBL and CNRS, 46 Allée d'Italie, Lyon, France
[2] IMPMC, MNHN, UPMC, UMR CNRS 7590, 61 rue Buffon, 75005 Paris, France
[3] School of Earth Sciences, University of Bristol, Wills Memorial Building, Queens Road, Bristol BS8 1RJ, UK

Corresponding author : bernard.bourdon@ens-lyon.fr

Abstract

The study of siderophile element isotope compositions in planetary mantles offers a new methodology to constrain the temperatures of core formation, provided there is an appropriate calibration of the temperature-dependence and possibly pressure-dependence of isotope fractionation between metal and silicate and of the metal-silicate partitioning for this element. In this review, we examine recent studies that have shown that Si, Fe, Mo, Cr, Cu, Ni, N and C could potentially be used to constrain the temperature of metal-silicate equilibration using single stage or continuous models of core formation, yielding contrasted results. Such an approach requires assumptions about the building blocks of the Earth and it is generally considered that the composition of some chondrites is representative of bulk Earth. This is obviously more complex for volatile elements such as Cu, N or C, as the isotope composition of the building blocks of the Earth could have been affected by thermal processing. On the basis of a chondritic bulk composition, one can estimate a temperature of core formation assuming a model for this process. If the metal-silicate equilibration is incomplete, as is likely the case for giant impacts, then the composition of the mantle of the impactor and the fraction of metal that equilibrate needs to be assessed carefully. It has been shown recently that the degree of equilibration will be a function of the metal-silicate partition coefficient and will be hence very different for Si, Cr, or Mo, an aspect that has not been considered in previous studies and may help explain differences in interpretation. In this context, the expected temperatures of equilibration are quite variable and are a function of the impactor's conditions of metal-silicate segregation. Another complication arises when considering continuous models of core formation: the most siderophile elements will be sensitive to the last episodes of core formation, while the budget of less siderophile elements will reflect its integrated accretion history (e.g. Cr or Si). A model including Si, Cr and Mo isotope data that takes into account these aspects

has been constructed and shown to be consistent with scenarii that were derived from siderophile element data.

Keywords: Stable isotope, core formation, isotope fractionation

1. Introduction

The formation of the core of planetesimals and planets is arguably the most dramatic event of planetary differentiation. Yet, it is also one of the most difficult processes to constrain as it is an early process whose direct signature is not always straightforward to disentangle and the inaccessibility of the core makes it difficult to constrain its composition. It is possible to provide indirect constraints on core formation by determining the abundance of refractory siderophile elements in the silicate portion of a planet. If one then assumes that the abundance of these refractory elements is roughly chondritic in the bulk planet, then one can directly infer the relative depletion of these elements in the mantle. This depletion may be explained by extraction of these elements to the metallic core. The next step is to make assumptions about how the metal segregated from the silicate and whether it equilibrated and at what pressures and temperatures. This commonly used approach has triggered a large number of experimental studies aimed at measuring directly the metal-silicate partition coefficients for a number of siderophile elements (e.g. Drake et al., 1989; O'Neill et al., 1998; Righter and Drake, 2000; Corgne et al., 2008; Mann et al., 2009; Siebert et al., 2011; Rubie et al. 2011; Fischer et al., 2015). For volatile elements, it is more difficult to constrain the bulk abundance, which complicates the determination of the degree of depletion in the silicate planet.

This approach has been very fruitful in attempting to determine the approximate pressure, temperature and oxygen fugacity (f_{O2}) conditions of core formation (e.g. Wade and Wood 2005; Siebert et al., 2013). However, there is a growing number of variables used in parameterizing experimentally determined partition coefficients and the models for core formation have grown in complexity. As core formation is a continuous process in large planetary bodies such as the Earth rather than a single discrete event, it is sensible to take this into account in models as the pressure and temperature of core formation are constantly evolving. This has been the case in most models produced over the past ten years (e.g. Wade and Wood, 2005; Rubie et al. 2011, 2015, Rudge et al. 2010) where the temperature, pressure and oxygen fugacity were chosen to evolve with time. The main conclusions of these studies is that the final pressure of metal-silicate separation in the Earth ranged between 30 and 70 GPa based mainly on Ni and Co data (Fischer et al. 2015) and that the f_{O2} could have evolved from more reducing (IW-4) to more

oxidized conditions (IW-2) towards the end of accretion (e.g. Wade and Wood 2005; Rubie et al. 2011, Fischer et al. 2015) to match the V and Cr data in particular but this last conclusion is disputed (e.g. Siebert et al. 2013). Unfortunately, there is no simple method to prescribe the variations of these parameters during accretion and these parameters are more often chosen using simple reasoning than carefully determined. One other key parameter is to determine the degree of equilibration of the metal and the silicate. As the Earth grows, the probability of large impacts generating high temperatures in the Earth increases and the large impacts are generally associated with 'core merging' whereby the metallic core of the differentiated impactor interacts little with the silicate mantle of the proto-Earth (Dahl and Stevenson 2010; Canup 2008; Deguen et al. 2014). In this case, models for core formation need to take into account this lack of equilibration (Halliday 2004; Rudge et al. 2010; Rubie et al. 2011; Deguen et al. 2014). For modelling large impacts with core merging, key input parameters are the temperatures and pressures of core formation in the embryos that accrete to the Earth (Rudge et al. 2010). When there is core merging, the effect of core formation on the accreting Earth can be viewed as transparent and it is the conditions in the embryos that determine the siderophile element contents of the Earth's mantle.

Despite the fact that core formation is a multi-step process, single stage models of core formation have still been presented and they have been argued to provide useful information. However, for elements with temperature-dependent metal-silicate partition coefficients, one should take into account that the recorded temperature is a function of the partition coefficients. This feature has been emphasized by Yu and Jacobsen (2012) who developed the concept of 'memory' for siderophile elements, expliciting the idea that more siderophile elements only record the last stages of accretion while less siderophile elements are sensitive to early stages as well. This was emphasized by a recent study of Dauphas (2017) focusing on the building blocks of the Earth during its accretion.

An independent means for constraining the temperature of core formation may be found in isotopes. Recently, it has been shown experimentally and sometimes theoretically that the stable isotopes of siderophile elements could fractionate between the metal and silicate phases (e.g. Roskosz et al., 2006; Georg et al. 2007; Roskosz et al., 2009; Shahar et al. 2011; Hin et al. 2012; 2013; 2014). Based on the temperature dependence of isotope fractionation, one could in principle infer an integrated temperature of metal-silicate fractionation over the period of core formation provided the element's concentration could be estimated independently. Unlike elemental partitioning that depends on temperature, pressure, oxygen fugacity, melt compositions and many other parameters, isotope fractionation depends on $1/T^2$ at temperatures

relevant to core formation and is seldomly influenced by other parameters. Thus, it should be a more specific temperature indicator. In this contribution, we shall review how this new tool could be used and the recent studies in this field are critically examined. A new quantitative model with which the current set of observations can be examined is then proposed.

2. Basic principles

Under equilibrium conditions, there can be a small yet measurable isotope fractionation for elements that partition between a metallic and a silicate phase. This fractionation could arise, among other effects, due to the fact that the degree of oxidation of that element is generally positive in the silicate while it is zero in the metallic phase. For example, Fe should have the +II or +III degree of oxidation while it is in the form Fe 0 in the metal. Thus, the following isotope exchange reaction can take place:

$$^{56}Fe + {}^{54}FeO \rightarrow {}^{56}FeO + {}^{54}Fe \qquad (1)$$

The equilibrium conditions can be written as :

$$\alpha = \frac{\left({}^{56}FeO\right)\left({}^{54}Fe\right)}{\left({}^{54}FeO\right)\left({}^{56}Fe\right)} \qquad (2)$$

where brackets indicate activities. This equilibrium constant has been shown by theoretical work to be temperature dependent (Bigeleisen and Mayer 1947; Urey, 1947) and the temperature dependence of isotope fractionation between metal and silicate at high temperature is generally expressed as:

$$\ln(\alpha) = \frac{A}{T^2} \qquad (3)$$

The parameter A is a constant that can be estimated either theoretically or using high temperature experiments. If one assumes that the bulk composition of the planet is known (usually one assumes a chondritic composition), then based on mass balance considerations, one can determine the temperature of metal-silicate equilibration by measuring the isotopic composition of iron in the mantle. A classical method to define Fe isotope composition is via the δ^{56}Fe notation which can be written as:

$$\delta^{56}Fe = \left(\frac{\left({}^{56}Fe/{}^{54}Fe\right)_{sample}}{\left({}^{56}Fe/{}^{54}Fe\right)_{reference}} - 1\right) \times 1000$$

First, the bulk Fe isotope composition of the Earth can be written as:

$$\delta^{56}Fe_{BE} = \delta^{56}Fe_{BSE}\left(1 - X_C^{Fe}\right) + \delta^{56}Fe_C X_C^{Fe} \qquad (4)$$

where X_C^{Fe} is the mass fraction of iron in the metallic core and the subscript BE and BSE indicate the bulk Earth and bulk Silicate Earth, respectively. This equation can be rewritten by including the hypothesis that the silicate mantle and the metallic core reached isotope equilibrium as stated in equation (1) and the fact that there is *chemical* equilibration between metal and silicate:

$$\delta^{56}Fe_{BE} - \delta^{56}Fe_{BSE} = \frac{X_C D_{Fe}}{1 - X_C + X_C D_{Fe}} \Delta^{56}Fe_{metal\_silicate}(T) \quad (5)$$

where X_C represents the mass fraction of the core, D_{Fe} is the metal-silicate partition coefficient of Fe, and $\Delta^{56}Fe_{metal\_silicate}$ is the isotopic difference between metal and silicate ($\delta^{56}Fe_{metal}$ - $\delta^{56}Fe_{silicate}$) which is approximately equal to 1000lnα. This equation shows that the net isotope fractionation between bulk Earth and bulk silicate Earth is a strong function of metal-silicate partitioning. For higher values of D_{Fe}, the isotope fractionation increases up to a maximum equal to $\Delta^{56}Fe_{metal\_silicate}(T)$. With this expression it becomes obvious that if one can determine the value of D_{Fe} independently, it is possible to determine the temperature of metal-silicate equilibration during core formation. This approach makes the simplistic assumption that core formation is well described by a single equilibration temperature corresponding to a single stage process. If it was a multiple stage process, then the derived temperature represents an integral of temperature over the duration of core formation.

This short introduction highlights the basic requirements for using an isotope approach to determine the conditions of core formation. First, one needs to make an hypothesis about the building blocks of a planet and it is generally assumed that chondrites are representing the most likely building blocks. Since the composition of chondrites is not always homogeneous among chondrite groups, this introduces an uncertainty and can be a matter of controversy (see section 4 for examples). For example, if chondrites have identical compositions, it is more likely that bulk planets are well represented by chondrites. One can also distinguish the case of refractory and volatile elements. For refractory elements, the isotope composition is more likely to be identical since thermal processes affecting the bulk composition of chondrites are less likely to play a role. There are various discussions regarding the building blocks of the Earth and it has been shown that the Earth's isotope composition could be well represented by enstatite chondrites for nucleosynthetic anomalies or by a mixture of chondrites and achondrites. However, this does not mean that the stable isotope compositions of bulk planets can be easily derived from these (a)chondrites, especially for volatile elements, which can be lost during

planetary accretion or during the protoplanetary stage. In addition to the bulk planetary composition, one needs to have a determination of the isotope composition of the bulk silicate Earth (BSE). In some cases, there is no or little isotope heterogeneity in all mantle-derived rocks while in other cases, it is necessary to understand the processes underlying the observed isotope variability to derive a BSE composition. Similar issues could arise in the case of siderophile element approach outlined above. Last, one needs to estimate the metal-silicate partition coefficient of the element of interest and this parameter is itself a function of temperature. This requires a degree of self consistency that can be checked a posteriori.

3. Determination of isotope fractionation between metal and silicate

3.1 Ab initio methods

Pioneering works by Urey (1947) and Bigeleisen and Mayer (1947) have shown that mass-dependent fractionation of isotopes is a function of their vibrational frequencies. More specifically, the equilibrium constant of an isotope exchange reaction (see equations (1) and (2) for an example reaction involving Fe) can be written in terms of the partition functions of the isotope species appearing in the reaction. Without going into the details of the derivation that can be found in numerous reviews (e.g. Schauble 2004; Young et al. 2015), it can be shown that the isotope fractionation factor relative to the atomic species (generally denominated β-factors) can be expressed as (Urey, 1947; Bigeleisen and Mayer, 1947):

$$\beta = 1 + \frac{h^2 \sum_i {\nu_{light}}^2 - {\nu_{heavy}}^2}{24 n k^2 T^2} \qquad (6)$$

in which h is Plank's constant, n is the number of atoms being substituted in the compound of interest, k is Stefan's constant, T is temperature in Kelvin and ν is the vibrational frequency of the isotope of interest. On this basis, theoretical estimates of isotope fractionation were made by Urey (1947) or Kieffer (1982) based on existing vibrational spectroscopic data. These data were not always available for other elements, thus other approaches are necessary. On the most general level, the idea is therefore to develop models that can predict the vibrational frequencies of minerals and melts that are substituted by isotopes. Once the frequencies have been estimated one can directly derive the isotope fractionation factor using equation (6).

The basic approach is to use density functional theory to determine the phonon density of states (PDOS) of the sublattice of the element of interest. This function describes the energy distribution of collective sub-lattice vibrations. The main goal is to calculate from first principles, the electronic structure of a molecule. The force constants that determine the

frequency of vibrations are then calculated as the second derivatives of the electronic energy as a function of atom displacement. It is not the purpose of this review to discuss the merits of various algorithms as such material can be found in Schauble (2004).

These calculations generally require a number of approximations which are briefly described here. First it is assumed that the electron density is sufficient to represent the wave function that is used in the Schrödinger equation. In this case, one makes use of a 'functional' (i.e. a function of a function) to represent the electron density. The energy of electrons is a function of the charge density and the charge density is itself a function of position. This energy is then calculated as a function of different terms:

$$E=E_{kin}(\rho)+E_{nuc}(\rho)+E_{e\_e}(\rho)+E_{exc}(\rho) \quad (7)$$

where ρ is the electron density which is itself a function of the distance to the nucleus r, E_{kin} is the kinetic energy, E_{nuc} the energy of interaction between the nucleus and the electrons, E_{e_e} the interaction energy between electrons and E_{exc} is the exchange correlation energy. This decomposition of the energy terms is made to avoid using direct electron interaction terms that make the equation insoluble. By expliciting the value of these functionals it is possible to solve the Schrödinger equation and derive the force constant for condensed phases. The difference in the various types of ab initio methods lie in the choice of expressions for the exchange correlation energy.

The applications of these *ab initio* methods for the case of metal-silicate differentiation have actually been rather limited, but they may expand in the future as their applications in the Earth Sciences become more widespread (see for example Blanchard et al., 2015; Shahar et al. 2016). The case of the metal-silicate equilibrium is a specific case as both phases of consideration are liquids. To a first approximation, the first published studies have used solid equivalents to represent the liquids (Georg et al. 2007; Shahar et al. 2016). For example, Georg et al. (2007) used Mg_2SiO_4 to represent the molten silicate and Fe_3Si to represent the molten alloy. In order to determine the energy shift associated with isotope substitution one calculates the phonon density of states (PDOS) of relevant phases. For the sake of simplicity, Georg et al. (2007) assumed that Si vibrated at the highest frequency of the observed spectrum, i.e. 10 THz in the Fe_3Si structure, corresponding to a Debye temperature of 366 K (Randl et al. 1995). In the case of metal silicate isotope exchange reactions, there are so far few cases where the isotope fractionation factors have been calculated with ab initio methods. It is obvious that these methods will provide a useful point of comparison with experimental approaches detailed in section 3.3.

3.2 Semi-empirical methods to estimate isotope fractionation factors

Alternative approaches that are less mathematically involved than *ab initio* methods are sometimes desirable. Young et al. (2009, 2015) and Sossi and O'Neill (2016) have used such an approach for Mg and Fe isotope fractionation among silicate minerals acknowledging that the mean value of the force constant associated with each bond suffices to estimate an approximate value of the isotope fractionation factor. This approach is valid only for crystalline solids but is very valuable as it can be cross-checked with experimental determinations. It is by no means universal but may prove useful if more reliable *ab initio* calculations or experiments have not been performed. For a crystalline solids, it is possible to calculate a value of the force constant as:

$$K_f = \frac{z_i z_j e^2 (1-n)}{4\pi\varepsilon_0 r_0^3} \quad (8)$$

where z_i and z_j represent the valence of a compound including a cation *i* and and anion *j*, *e* the charge of the electron, *n* is a Born-Mayer constant for repulsion (Young et al., 2015, adopted a value of 12), r_0 is the equilibrium interatomic distance, and ε_0 the vacuum permittivity. Various attempts have been made to take into account the fact that the bonds can be partly covalent in which case the value of the valence is lower than z_i or z_j. Similarly, since the charge is distributed between a number of nearest neighbors, the charge can be divided by the coordination for a given site (Young et al. 2009). It turns out that from an empirical viewpoint (Young et al. 2015), the equation gives more reliable estimates of the force constant than more complex formulations.

The approach above is valid for an ionic crystal but it fails when metals are considered. In this case, an alternative approach is possible, although it only applies to pure metals. It is based on a simplified treatment of vibrations in solids as defined in the Debye model. This model assumes that solids can be treated as coupled harmonic oscillators whose mean vibration frequency can be calculated. The parameter used to characterize the system of oscillators is the Debye temperature. Based on this temperature, it is possible to estimate the force constant (Gupta 1972):

$$K_f = \frac{m k^2 \theta_D^2}{4h^2} \quad (9)$$

Where θ_D is the Debye temperature of the metal, *k* the Boltzmann constant, *h* the reduced Planck constant, and *m* is the mass in kg. Polyakov (2005) used this approach for tin isotopes to directly relate its Debye temperature to a force constant and thereby calculate the tin isotope

fractionation factor. The force constant is then directly related to the maximum vibration frequency by:

$$\omega_{\max}^2 = \frac{4K_f}{m} \qquad (10)$$

Thus, a knowledge of this frequency is sufficient to estimate the force constant. If one assumes that the nearest neighbors are the most important in defining an effective force constant the simplified approach described above should help in determining an approximate value of isotope fractionation factors between an oxide containing the metal of interest and its metallic counterpart (see example with Fe isotopes, Figure 1). This example shows that this approach is valid but the element of interest will be a trace in iron rather than in the pure metal and this may introduce some bias.

3.3 Metal-silicate equilibrium experiments

3.3.1 Basic requirements and techniques

In order to determine the equilibrium isotope fractionation factors for the elements of interest, it is important to design experiments that will reproduce reliably the conditions of metal-silicate equilibration in terms of chemical composition, while allowing for practically manageable experiments. Most experiments are performed in a one-atmosphere furnace or piston cylinder apparatus (e.g. Roskosz et al., 2006; Poitrasson et al., 2009; Hin et al. 2013, 2014, Shahar et al., 2015; Lazar et al., 2012; Bonnand et al., 2016), although multi-anvil assemblies have also been used (e.g. Poitrasson et al. 2009 ; Williams et al. 2012). There are several potential problems in designing such experiments: (1) the capsule or loop materials used for the experiments can react with the charge, thereby creating open system behaviour. (2) The duration and/or temperature of the experiments have to be adjusted so as to reach chemical and isotopic equilibrium. However, the choices for temperature (and thereby duration) are influenced by the trade-off that higher temperatures lead to faster equilibration, but also to smaller isotope fractionation (see equation (6)). (3) There must be an easy method to separate the metal from the silicate if the isotope composition of the tracer is not measured in situ. Alternatively, if the isotope composition is determined in situ, then the metal and silicate must have well separated domains, with no inclusions. This problem is particularly acute when the metal-silicate partition coefficient is very different from unity, such that there are large difference in concentrations between the two phases, leading to high sensitivity to cross-contamination. (4) In order to reliably calibrate the temperature dependence of isotope

fractionation, it is desirable to design experiments at different temperatures, although in principle a single datum obtained at a given temperature is sufficient to determine the value of A in equation (3).

As in standard petrology experiments, it is important to control the temperature, the oxygen fugacity, or other relevant parameters as any change in the parameters affecting the partitioning may lead to a diffusive fractionation that may further delay the attainment of the isotopic equilibrium (e.g. Richter et al., 2009; Roskosz et al., 2006).

As core formation in terrestrial planetary bodies frequently involves temperatures >1000°C and pressures >0.5 GPa (unless core formation took place in planetesimals that accreted with no further metal-silicate equilibration), experimental equipment needs to reach such temperature and pressure conditions. High pressures are generally obtained by exerting a force on a relatively small area in which the sample resides, so the higher the obtained pressures, the smaller the samples. This feature currently limits our pressure range for calibrating mass-dependent isotope fractionation factors, because solution MC-ICPMS (multi-collector inductively coupled plasma mass spectrometry) is generally the preferred technique for analysis. This is a 'bulk', as opposed to *in situ* analysis technique that mostly requires tens to hundreds of nanogram of the element of interest. Most studies have therefore performed high pressure experiments with a piston cylinder apparatus (Poitrasson et al., 2009; Shahar et al., 2009; Shahar et al., 2011; Hin et al., 2012; Lazar et al., 2012; Hin et al., 2013; Hin et al., 2014; Shahar et al., 2015), which generally reaches a pressure range of 0.5-3.8 GPa and temperatures up to ~2700°C with sample volumes commonly <160 mm^3, which is equivalent to <500 mg sample. Experiments have also been performed with a multi-anvil apparatus (Poitrasson et al., 2009; Shahar et al., 2011; Williams et al., 2012; Kempl et al., 2016), which can achieve pressures of ~3-25 GPa and temperatures similar to those in piston cylinders with sample volumes <16 mm^3, or <50 mg. Laser-heated diamond anvil cell (>200 GPa; >3000°C; samples <0.14 mm^3 or <0.4 mg) have thus far only been used for *in situ* analysis (see below). Alternatively, controlled-atmosphere furnaces (1-atm pressure, generally up to ~1800°C) have been used (Cohen et al., 2006; Roskosz et al., 2006) because they uniquely provide controlled oxygen fugacity and, from an isotope geochemists point of view, virtually unlimited sample material. It should be mentioned also that alternative methods based on industrial blast furnaces have also been used to attempt to determine isotope fractionation factors (Kempl et al. 2013; Milot et al. 2016). These results are probably indicative of the order of magnitude and direction of isotope fractionation but it is difficult to use them as firm determinations due to a lack of

control on the experimental conditions associated with chemical disequilibrium and poorly controlled reservoir compositions.

Controlled-atmosphere furnaces are relatively straightforward to use (e.g. Edgar 1973; Huebner 1987). For metal-silicate experiments, the sample powder is commonly placed in a crucible and hung from the insertion rod on a metal wire or ceramic ring inside a tubular furnace. At the end of the experiment, this ring or wire is released from the rod so the sample can drop through an opening into a cold environment (e.g. a water bath) to quench the sample. Oxygen fugacity in these furnaces is controlled by flushing a desired mixture of gases (most commonly CO_2-H_2 or CO_2-CO mixtures; fluxes commonly of the order of mL min^{-1}) through the alumina gas-tight tube located inside the heated zone of the furnace. Oxygen abundance in the chosen flux sets the oxygen fugacity of the experiment. A relative fugacity between ~4 log units below the iron-wüstite buffer (or fO_2 of ~10^{-13} at 1500°C) and ~7 log units above this buffer (fO_2 ~10^{-2} at 1500°C) can routinely be achieved by varying the flux ratios of those gases. A deleterious consequence of this setup is that experimental charges are usually open systems with respect to gases. This effect may be exacerbated by the low f_{O2} required to stabilize Fe metal, because many elements (e.g. Cu and Zn) become increasingly volatile at lower fO_2. This feature can lead to partial vaporization and thereby kinetic Rayleigh isotope fractionation, which needs to be considered if the element of interest is volatile under the chosen experimental conditions.

Piston cylinder and multi-anvil methods are more laborious because in addition to sample capsules, non-reusable heaters and fillers need to be assembled for each experiment and then carefully placed inside the stacked metals of the apparatus. Additionally, the smaller materials become increasingly difficult to handle and sample capsules need to be sealed because gases cannot be fluxed through these apparatuses to control oxygen fugacity. This fugacity is therefore set by the oxides and metals inside the capsule and/or their exchange with the capsule material (e.g. Eugster, 1957; Chou, 1987; Matjuschkin et al. 2015). It is therefore difficult to attain a predetermined value of this thermodynamical parameter in contrast to controlled-atmosphere furnaces. Heat is produced by running an electrical current through a heater that is usually made of graphite, or of LaCrO3 in experiments above the graphite stability field. Quenching then occurs by switching off the power.

3.3.2 Pitfalls: Unwanted reactions, open system behavior, thermal diffusion

During an experiment, separation of immiscible phases such as metal and silicate occurs due to surface tension and gravitational sorting. In conventional static experiments these processes

rarely generate a single sphere containing 100% of the metal present in the sample. A word of caution may be necessary here. Even if complete separation appears achieved, very small nuggets of metal commonly persist suspended in the silicate phase (e.g. see discussion in Médard et al., 2015), although their abundance appears restricted when using starting powders with equilibrium metal and silicate weight ratios and compositions (Médard et al., 2015). Nonetheless, these nuggets are mostly problematic for highly siderophile elements but not for moderately siderophile elements (which are the focus of this study) because cross-contamination is a mass balance effect. It thus depends on the distribution of isotopes as well as of the element as a whole: a strong contrast in both types of distributions will readily contaminate the phase with the low elemental abundance generating an underestimation of the isotope fractionation factor beyond analytical errors. Obviously, when two phases have identical elemental and isotopic abundances, cross contamination plays no role, but the isotope fractionation factor is often investigated without prior knowledge of its magnitude. Monitoring of cross-contamination could be done by doping the experiment with elements that have a near-quantitative affinity for either silicate or metal. Nonetheless, owing to cross-contamination issues, conventional experiments require laborious phase separation procedures (e.g. Poitrasson et al., 2009). Micro-sampling techniques such as micro-drilling (e.g. Charlier et al. 2006) can be employed. Alternatively, the entire sample containing mingled metal and silicate phases needs to be removed from the capsule material, followed by crushing and magnetic separation and/or hand-picking under a binocular microscope. It may be possible to correct a posteriori for the effect of contamination of one phase by another if the isotope composition of the contaminating phase can be determined separately.

Additionally to physical phase separation, chemical separation is principally also possible, e.g. by using dilute hydrofluoric acid to dissolve silicate glass without attacking the metal phase. Such preferential dissolution has been quite common in studies of mass-independent isotope compositions, e.g. to investigate carrier phases of isotopic anomalies (e.g. Rotaru et al., 1992). Chemical separation (e.g. Williams et al., 2012), however, is not as common for mass-dependent isotope analyses, because of the potential for mass-dependent isotope fractionation due to leaching or partial dissolution of the contaminant phase. Since these can result in kinetic or low temperature equilibrium isotope fractionation (e.g. see discussion in Poitrasson et al. 2009), it potentially overwhelms the much smaller high temperature metal-silicate fractionation. Chemical separation therefore requires careful investigation of such isotope effects for the investigated isotope system (see Poitrasson et al., 2009 for an example with Fe isotopes).

To aid the physical separation of immiscible phases, a centrifuging furnace (Roeder and Dixon, 1977) and piston cylinder (Schmidt et al., 2006) have been designed in some experimental petrology laboratories. This is particularly effective for liquid systems, as is often the case in metal-silicate experiments mimicking core formation. Despite lacking a gas controlled environment, a centrifuging furnace has proven particularly useful for studying highly siderophile element partitioning (Brenan, 2008). Unlike the centrifuging furnace, the centrifuging piston cylinder has been used to study mass-dependent isotope fractionation factors between metal and silicate. Since the metal and silicate can be physically separated it is possible to use a 'bulk' analysis technique for determining isotope ratios (which is easier to calibrate than in situ methods) and it has proven particularly useful for the moderately siderophile element molybdenum (Hin et al., 2013). However, compared to static experiments, it also helps separation of metal and silicate after the experiment prior to dissolution. As detailed in Hin et al. (2012) two bulk pieces can be removed by sawing and once cleaned from surface contamination, silicate-free metal and metal-free silicate samples have thus been obtained for dissolution, ion exchange chromatography and analysis.

The nature of the crucibles in which metal-silicate samples are held, are major issue when investigating equilibrium isotope fractionation factors. There are several materials that are (virtually) inert to either silicate or metal, but none that are inert to both. Graphite, MgO and to lesser extent boron nitride (BN) have become the most popular choices of capsule material, choices that have mostly been adopted from element partitioning experiments between metal and silicate liquids. Graphite, for instance, has limited solubility of usually <10 wt% in metal (Lord et al., 2009) and silicate (as CO_2) (Mysen et al., 1976). Similarly, nitrogen solubility remains below ~10 wt% in liquid Fe-Ni alloy and below ~0.5 wt% in basaltic silicate liquid (Roskosz et al., 2013). In contrast, boron and MgO are virtually inert to metal yet react with silicate. While B is a trace element in magmatic system, its addition from capsule material may modify the bonding environment of metal oxides (Wang and Stebbins 1998). This reactiveness can be limited by increasing their contents in the starting mixture and reducing run durations of the experiment to a minimum. However, as suggested in Hin et al. (2013) there can be conditions under which the continually changing silicate composition during an experiment continuously affects the solubility of the element of interest. This transient state inhibits isotopic equilibration if the rate of element transfer from metal to silicate (or vice versa) exceeds the rate of isotope equilibration. This issue is probably particularly relevant to elements whose solubility is sensitive to compositional changes and characterized by low diffusivities, such as

for highly charged elements in silicate liquids (Ellison and Hess, 1986; Hillgren et al., 1996). While we draw the attention to these features, a quantitative assessment remains difficult due to poor knowledge of kinetic parameters. Similar equilibration issues may arise if the element of interest interacts with the capsule material, e.g. Fe diffusion into an MgO capsule to form ferropericlase. Such setups require careful investigation of isotope equilibration (see below).

Capsule solubility in metal or silicate and hence the choice of capsule material is also a matter of concern if isotope fractionation factors are dependent on composition. The extent of such compositional dependence is still a matter of debate. There is ample evidence (Ma, 2001; Wagner, 1952) that elemental distributions between metal and silicate are strongly affected by the composition of either phase (e.g. carbon solubility in metal due to the use of graphite capsules). Initial investigations showed a remarkable resilience of isotope fractionation factors towards compositional variations in Fe-based metals and (ultra)mafic silicates. For instance, multiple studies observed no change in Si isotope fractionation between metal and silicate liquids in C-bearing and C-free systems (Hin et al., 2014; Shahar et al., 2011). Similarly, comparison of Sn-bearing and Sn-free systems yielded identical Mo and Si isotope fractionation factors (Hin et al., 2013; Hin et al., 2014). A study of a wide range of silicate melt compositions from basaltic to rhyolitic, however, has shown that over that compositional range, iron isotope fractionation is affected by changes in coordination state as well as changes in the relative mineral-melt partitioning of $Fe^{3+}$and Fe^{2+} (Dauphas et al. 2014). Additionally, recent contributions (e.g. Shahar et al., 2015, Liu et al., 2017) that investigated metal composition effects on Fe isotope fractionation in more detail imply that such effects occur, although some findings are still a matter of debate (see section 4.5 on Fe isotopes for more details).

Another potential issue when experimentally determining isotope fractionation factors is that isotopes can fractionate along temperature gradients due to the Soret effect (Kyser et al., 1998): for example, Mg isotope variations of several ‰ have been observed in piston cylinder experiments with a temperature gradient of ~150°C between the hot and cold ends of the capsule (Richter et al., 2008). Temperature gradients in the hot part of (gas controlled) furnaces are so small that such a thermal effect is not a matter of concern over the dimensions of the sample. Temperature calibrations in piston cylinders show substantially steeper temperature gradients. However, these calibrations also show that temperature differences between the hottest and coldest part of a capsule can be reduced to a likely insignificant <9°C by carefully centering the capsule in the hotspot of the assembly and by restricting the sample length to <~4 mm (e.g. Poitrasson et al., 2009; Hin et al., 2012; Watson et al., 2002). The temperature gradients in

multi-anvil experiments, however, are more than double for the lowest pressure (18/11) assemblies and rapidly steepen for higher pressure assemblies (van Westrenen et al., 2003). Unless technical advances reduce these gradients, multi-anvil experiments will have to be performed keeping in mind the possibility of isotope fractionation by thermal diffusion. The short run durations (minutes) required for equilibration of liquid metal – liquid silicate experiments at temperatures >2000°C may fortuitously minimise Soret isotope effects because such effects appear to need tens of hours to develop (Richter et al., 2009). Otherwise, multi-anvil run products require careful sampling of adjacent metal and silicate pairs. Such sampling should avoid the effects of thermal diffusion as locally metal and silicate should be equilibrated and not affected by temperature gradients.

Equilibration is an important aspect of experiments aimed at calibrating equilibrium isotope fractionation factors. Time series are the most common approach to ensure equilibrium is achieved, i.e. if the distribution of isotopes or elements between the studied phases does not change with increased experimental run duration, equilibrium ought to have been achieved (Figure 2). Observations show that run durations of five seconds suffice to achieve elemental equilibrium in liquid metal – liquid silicate experiments at 2300 K (Thibault and Walter, 1995). Such equilibration times need not be identical for isotopic studies because isotopes may have slightly different chemical potentials driving the rates of their reactions (Lesher, 1990; Van der Laan et al., 1994). However, various studies on a variety of elements indicate similarly short isotopic equilibration times of the order of minutes to <2 hours, depending on temperature (Hin et al., 2013; Hin et al., 2014; Hin et al., 2012; Poitrasson et al., 2009; Shahar et al., 2011). Such fast equilibration is likely related to high diffusion coefficients in liquids at high temperatures and to short diffusion distances, particularly at the onset of melting of the finely ground and homogenised samples.

If one or more of the phases is in solid state, reaching equilibrium within reasonable experimental run durations may be difficult because of slower diffusion. This issue can be circumvented by designing the experiment such that the faster process of (re-)crystallization of the solid phase(s) occurs. Altogether this can force isotope equilibrium to take place despite the presence of a solids with slow exchange kinetics. This process can be induced by exceeding the liquidus temperature prior to dropping the temperature to that desired for the experiment or by using starting material that has a different crystal structure than at the pressure and temperature of the experiment, by phase reactions that form the mineral phase used for equilibration by reaction with a silicate melt (e.g. Fe isotopes between pyrrhotite and silicate melt, Schuessler

et al., 2007), or by equilibration with a fluid to speed up isotope exchange kinetics (see Sossi and O'Neill, 2017, for an example with silicate minerals).

3.3.3 Demonstrating isotopic equilibrium and a discussion of the three- isotope method

Alternatively to time series, a potentially very powerful technique, referred to as the "three-isotope method" (Matsuhisa et al., 1978; Northrop and Clayton, 1966; Shahar et al., 2008) has been used to extrapolate isotopic compositions of a series of unequilibrated experiments to their equilibrium isotope compositions and eventually to obtain the equilibrium fractionation factors. Although this method of adding an isotope spike to one of the phases in the starting material has also been used in liquid metal – liquid silicate experiments, its use in such experiments is found mostly in investigating whether chemical exchange indeed occurred and whether loss or gain of isotopes occurred during the experiment, e.g. by exchange with the capsule material. This is more readily investigated with an isotope spike because it induces easily detected differences between the phases in the starting material, which may not be present when natural isotope compositions are used. The three-isotope method has recently been discussed in a review by Young et al. (2015), so the reader is referred to that work and original contributions cited above for more details. With the three-isotope approach it is possible to infer the isotopic difference between two phases ($\Delta_{x\text{-}y}$ defined as $10^3 \times \ln(\alpha_{x\_y})$, where α is the fractionation factor between phases x and y, see equation (2)) by using the trajectory of isotope composition in isotope space. The trajectories are assumed to be linear and provided the bulk composition of the system is known, one can infer the value of $\Delta_{x\text{-}y}$ by calculating the intersection of the isotope trajectory of the metal phase (or the silicate phase) with the mass-dependent fractionation line that is pinned to the bulk composition, which is itself known from measurements of the bulk starting material. For example, Shahar et al. (2011) and Lazar et al. (2012) used this technique to determine the $\Delta_{x\text{-}y}$ -value starting from compositions that had been doped in a specific isotope.

A recent study focusing on O and C isotopes (Cao and Bao 2017) has also reviewed the three isotope technique and pointed out numerous artifacts related to kinetic effects for these systems. In this review, we have examined the validity of this approach from a theoretical viewpoint. We have used two theoretical models to investigate the shape of the trajectories. First, Criss et al. (1987) have shown that the isotope composition of a two-phase system would follow first order kinetics:

$$\frac{dR_{met}}{dt} = k_1\left(\alpha_{eq} R_{sil} - R_{met}\right) \qquad (11)$$

where k_1 is kinetic constant for a metallic phase, R_{met}, R_{sil} are the isotope ratios in a metallic phase and silicate phase respectively and α_{eq} is the isotope fractionation factor between metal and silicate. The solution of this equation is:

$$R_{met}(t) = R_{met}^{eq} + \left(R_{met}^{0} - R_{met}^{eq}\right)\left(1 - e^{-\left(\frac{\alpha_{eq}}{1-fmet}+1\right)k_1 t}\right) \qquad (12)$$

where f_{met} is the fraction of the element of interest in the metallic phase and superscripts 0 and eq refer to initial state and equilibrium, respectively. The equation for R_{sil} can be deduced by mass balance using the following equation:

$$R_{sil} = (R_{mix} - f_{met} R_{met})/(1 - f_{met}) \qquad (13)$$

These equations are valid only if the fraction of the element in the metallic phase is fixed, which is generally not the case. If f_{met} evolves during the isotope equilibration reaction, indicating that the metal and silicate are initially out of *chemical* equilibrium, then the evolution of R_{met} and R_{sil} can be non-linear and their time evolution needs to be integrated numerically. In this case, as shown by Cao and Bao (2017), the following equation can be used:

$$\frac{dR_{met}}{dt} = \frac{k_f \alpha_{eq}}{1 - f_{met}} R_{mix} - \frac{k_f (f_{met}\alpha_{eq} + 1 - f_{met})}{1 - f_{met}} R_{met} \qquad (14)$$

where k_f is a kinetic constant for the forward reaction. These equations make no assumption about the driving mechanism for isotope equilibration. A simplistic method is to scale the value of the kinetic constants with the square root of the mass of isotope ratios to simulate the effect of kinetic fractionation. We have integrated numerically equation (14) assuming that the value of f_{met} evolved with the following equation (corresponding to first-order kinetics):

$$f_{met} = f_{met}^{0} + \left(f_{eq} - f_{met}^{0}\right)e^{-t/\tau} \qquad (15)$$

Where τ is a time scale for chemical equilibration. The linearity of trajectories is a function of how far from equilibrium the initial system is. As shown in Figure 3, when the system is close to equilibrium $f_{met}^{0} \sim f_{eq}$, then the trajectories are linear, whereas they can be non linear when the system is initially out of chemical equilibrium (Figure 3). The non-linearity is also a function of how far from the mass fractionation line of the system the initial metal and silicate phases are. These features are also discussed semi-quantitatively in Cao and Bao (2017) for oxygen isotope chemical reactions. This simplistic approach further highlights the conclusions of Cao and Bao (2017) regarding the three isotope methods and suggests a good characteriziation of reaction kinetics is necessary.

In the case of metal-silicate experiments the most likely process for equilibration, in the absence of reactions (f_{met}=constant in this case) will be diffusion. Thus, we have examined the isotope trajectories in the case of equilibration via diffusion. Cole et al (1983) have shown that in the case of a phase with a slower diffusion (i.e. in the silicate), the equation for the isotope ratio of interest in the silicate phase as a function of time should be:

$$\frac{R_{sil}(t)-R_{sil}^{eq}}{R_{sil}^{0}-R_{sil}^{eq}}=\sum_{n=1}^{\infty}\frac{6\beta(\beta+1)e^{Dq_n^2t/a^2}}{9+9\beta+q_n^2\beta^2} \quad (16)$$

where β is the metal to silicate volume ratio, D the diffusion coefficient of the isotope in the silicate, a the radius of spherical grains and q_n are the non-zero values of the following equation:

$$\tan(q_n)=\frac{3q_n}{3+\beta q_n^2} \quad (17)$$

The value of R_{sil}^{eq} is calculated with the following equation:

$$R_{sil}^{eq}=\frac{R_{bulk}}{\alpha_{m\_sil}(1-X_{sil})+X_{sil}} \quad (18)$$

with X_{sil} being the mass fraction of the element in the silicate. Assuming that the system is closed, one can infer the isotope composition of the metal phase (R_m) as:

$$R_m(t)=\frac{R_{bulk}-X_{sil}\times R_{sil}(t)}{1-X_{sil}} \quad (19)$$

If we assume that diffusion for a given isotope in the silicate melt scales as a power m of the mass of this isotope (previously assumed to be equal to 0.5), then the trajectories of equilibration between metal and silicate can be calculated. The trajectories for diffusive equilibration are shown for various values of m (Figure 4) and it is obvious that they are linear unless the values of m are unrealistically large (e.g. 5). This means that diffusive equilibration should lead to conditions where the three isotope method is valid. A good check is that the slope of the metal silicate pair should be approximately (57-54)/(56-54)=1.5 in the case of iron isotopes.

In summary, the application of the three isotope method to metal-silicate equilibrium is not so straight forward as non-linear trajectories can potentially be obtained in which case a linear extrapolation of the equilibrium isotope fractionation factor is difficult. The conditions for having non-linear trajectories have been outlined in Bao and Cao (2017) and we have shown quantitatively here that in the particular case of a reaction leading to a net transfer from one phase to another could produce such effect. This does not mean that this approach is invalid but that special care must be taken.

3.4 The application of NRIXS to constrain metal-silicate isotope equilibria

Instead of using *ab initio* calculations to model the phonon density of states of a phase, it can also be measured in some cases. The Nuclear Resonant Inelastic X-ray Scattering (NRIXS) technique provides direct access to the partial and projected phonon DOS for the resonant isotopes only (Kohn et al., 1998, Sturhahn and Kohn, 1999). This complete isotope selectivity is truly unique among techniques for the study of vibrational properties of solids. It can be a disadvantage to be restricted to vibrational information only from nuclear resonant isotopes in a multicomponent system. But this is also precisely what makes NRIXS suitable for isotope geochemistry applications because the derived properties, such as the mean force constant (K_f), fully yet selectively characterize the vibrational behavior of the element of interest. Equilibrium isotope fractionation factors characterizing metal-silicate equilibrium can be derived from the value of K_f measured on nuclear resonant isotopes because K_f is the second-order derivative of the interaction potential, which is constant and does not depend on the mass of the isotope for a harmonic oscillator (Lipkin, 1995). Therefore, the β-factors are related to the mean force constant of the harmonic oscillators holding the element in place (Bigeleisen and Mayer, 1947),

$$1000 ln\beta_{i_2/i_1} = 1000\frac{\hbar^2}{8(kT)^2}K_f\left(\frac{1}{m_1}-\frac{1}{m_2}\right) \quad (20)$$

where $\hbar$ is the reduced Planck constant ($h/2\pi$), k is the Boltzmann constant, T is the temperature, K_f is the average force constant (N/m^2), and m_1 and m_2 are the masses of the two isotopes i_1 and i_2, respectively. Note that the force constant simply corresponds to the force constant of a harmonic spring that is used to represent vibrations in solids.

Practically-speaking, NRIXS relies on the fact that some nuclei such as ^{57}Fe or ^{119}Sn have low lying nuclear excited states that can be populated by X-ray photons at a nominal resonance energy (14.42125 keV in the case of iron). This elastic transition itself does not provide the necessary information about the sublattice. However, when the energy of the incident X-ray beam is slightly lower than the nominal resonance, some lattice vibrations can fill the gap and provide some extra energy (in the form of phonons) to allow the nuclear transition to an excited state to occur. Conversely, when the energy of the incident X-rays is slightly higher than the resonance, the transition occurs and the extra energy is transferred to the target (in the form of

phonons). These processes are known as phonon annihilation and creation respectively. Consequently, by measuring the flux of scattered X-rays as a function of the incident X-ray energy (the scattering probability, S(E)), the vibrational properties of the sublattice is probed. This is precisely what is required to extract equilibrium fractionation factors (Bigeleisen and Mayer, 1947; Urey, 1947; Dauphas et al., 2012).

Two approaches have been proposed to retrieve the β-factors once scattering probabilities have been obtained. Polyakov et al. (2007) initially used the kinetic energy and first order perturbation theory to calculate the β-factors from the PDOS of the iron sublattice. Dauphas et al. (2012) derived instead the mean force constant of the sublattice from the raw scattering probabilities (S(E)). The two approaches have been found mathematically equivalent but the error propagation is more straightforward when the second approach is followed. The details of the data processing is discussed elsewhere (Dauphas et al., 2014; Blanchard et al., 2015). Nonetheless, from a theoretical viewpoint, in the context of quadratic potentials, the mean force constant can be derived from the third order moment of the scattering probability (Lipkin, 1995; Sturhahn, 2004):

$$\langle F \rangle = \frac{M}{E_R \hbar^2} \int_{-\infty}^{+\infty} \left(E - E_R\right)^3 S(E)\, \mathrm{d}E, \qquad (21)$$

where $E_R = {E_0}^2 / 2Mc^2$ is the free recoil energy (E_0 is energy of nuclear resonance and c is the speed of light in vacuum), M is the mass of the nuclide, $S(E)$ is the scattering probability (*i.e.*, the raw NRIXS spectrum), and E stands for energy. Since the force constants are integrals that are weighted by the cube of the energy, even small bumps in the high-energy tails of S(E) or in the PDOS can have sufficient weight to affect the value of the force constant and hence the β-factors. As these tails are characterized by low counting statistics, determining K_f for applications to isotope geochemistry is therefore particularly challenging as this requires broad energy scans and long acquisition times.

Experimental details are beyond the scope of this review (see for instance Dauphas et al., 2012; 2014). However, one needs to provide words of caution when NRIXS spectra are collected for geochemical applications. Before 2012, geochemical applications of this spectroscopy essentially focused on the determination of the Debye sound velocity from which compression and shear velocities where extracted (Sturhahn and Jackson 2007). For such applications only the low energy range of the spectrum (where the signal is intense) was needed. For isotope geochemistry, the entire energy range needs to be accurately sampled. The experimental

consequence is that the energy of the incident beam has to be varied within a typical range of -200 to +200 meV around the nominal resonance energy. Previously published spectra are often very noisy at high energies and sometimes, the measurements where truncated before the signal reached zero at the high energy tail. Therefore, these spectra must be considered with caution as discussed below.

Thus far, the application of NRIXS spectroscopy in isotope geochemistry has been restricted to iron. The following review therefore only focuses on this isotopic system. Recent studies of Fe isotope fractionation between minerals can be found in Roskosz et al., (2015) and Blanchard et al. (2015). Direct comparison between *ab initio* and experimental studies was performed. For goethite, the β-factor calculated from the revised NRIXS data of Dauphas et al. (2012) was found to be overall consistent yet slightly higher than the first principle calculations (Blanchard et al., 2015). The system olivine-spinel was also tested (Roskosz et al., 2015). Here, NRIXS data collected on an olivine Fo_{82} and a spinel with a Fe^{3+}/Fe_{tot} relevant to magnetite were compared with experimental data collected on the magnetite-fayalite couple (Shahar et al., 2008) and with β-factors extracted from Mössbauer spectroscopy (e.g. Polyakov and Mineev 2000). The NRIXS results were within error of the experimental data (0.04-0.08 ‰). There was also good agreement with previous spectroscopic studies as far as equilibrium fractionation factors (i.e. the difference between two β-factors) were concerned but the individual β-factors were found to be very different. Such disagreements between β-factors of a given mineral is also common in the field of *ab initio* calculation studies. Without knowledge of the true value, this observation demonstrates that self-consistent datasets are needed to derive reliable isotope fractionation factors. Combining data collected by very different methods must be done with extreme caution.

The first prediction of metal-silicate iron isotope partitioning based on NRIXS spectra, suggested that core-mantle differentiation would leave an imprint on the iron isotope signature of the Earth (Polyakov, 2009). This study suggested that the enrichment of terrestrial and lunar basalts in heavy iron isotopes relative to those from Mars or Vesta is due to high-pressure equilibrium iron isotope fractionation between silicates (dominated by Fe^{2+} bearing post-perovskite) and metal (0.1‰ at 3000°C). However, this important conclusion was derived from available literature spectra of samples synthesized at high pressure in a diamond anvil cell in the stability field of post-perovskite. These measurements were carried out to derive sound-

velocities of post-perovskite. Consequently, the high-energy tail of the spectra was not resolved enough to allow these data to be safely used to derive equilibrium isotope fractionation factors. Later, a comprehensive compilation of available data on metals, silicates and sulfides was published (Dauphas et al., 2012). Keeping in mind that some of these results may also suffer from a poor spectral resolution, the authors demonstrated that no significant fractionation should be expected at high temperature and low pressure between iron metal and silicates (Dauphas et al., 2014), in agreement with Poitrasson et al. (2009) and Hin et al. (2012). This compilation did not consider the hypothetical effect of pressure on the fractionation factors as in the earlier work of Polyakov (2009).

More recently, two experimental studies tackled the question of the isotopic imprint of metal-silicate equilibration during core formation by measuring, *in situ*, at high-pressure, the effect of alloying elements on the β-factors of metallic iron-based alloys. Shahar et al. (2016) measured the NRIXS spectra of FeO, Fe_3C and FeH_x. Combined with first-principle calculations on Fe-bearing bridgmanite, these results suggested that pressure may have a direct effect on the fractionation factors because of the contrasted stiffening of bonds from one mineral to another with increasing pressure. This theoretically expected result provided the basis to conclude that FeH_x and Fe_3C were probably not major components making the Earth' core. Liu et al. (2017) analyzed more realistic metal alloys in the context of planetary cores (namely, $Fe_{86.8}Ni_{8.6}Si_{4.6}$, $Fe_{92}Ni_8$, $Fe_{85}Si_{15}$ and Fe_3S) and a fully reduced basaltic glass up to 65 GPa (and 135 GPa for alloys). Considering their data set for the basaltic glass instead of the calculation for bridgmanite, Liu et al. provided a self-consistent dataset including previous NRIXS results from Shahar et al. (2016). Although their results were generally consistent with Shahar et al. (2016), in detail the pressure effects on the fractionation factors were found to be much smaller and even smaller fractionation factors were found between alloys and melts. They could not resolve any significant pressure effects on the equilibrium fractionation factors at pressures and temperatures relevant for the Earth's core formation. These NRIXS data imply that iron isotopes may not be a good proxy for determining the composition of Earth's core or the thermodynamic conditions under which it formed. Nonetheless, the present limitations of the spectroscopic methods are such that more subtle effects of anharmonicity, of spin transitions or of the difference between molten and quenched materials may have remained unresolved so far.

4. A review of recent applications of metal isotopes to constrain core formation

In this section, the results obtained for a number of isotope systems are examined by order of increasing atomic numbers. Although some other elements (e.g. V, S, W, Ga and Ge) have been also utilized as tracers of core formation, they have not been included in this review because each of these elements has currently only been investigated once.

4.1 Carbon isotopes

Carbon is of particular interest in this list as carbon is a light element whose presence has been suggested to explain the density deficit of the outer core (e.g. Poirier 1994). The carbon isotope composition of the mantle has been the focus of much research as it has been used as a tool to understand the formation of diamonds. There is a bimodal distribution in the isotope composition of C in the mantle. It has been argued that the value representative of the primitive mantle is $\delta^{13}C$= -5±5‰ while the other mode (-25±6‰) is due to subduction recycling (Wood et al. 2013). In contrast, there is a large range in $\delta^{13}C$ in chondrites with values ranging between -25 to +4 ‰ (Grady and Wright 2003). A comparison with other planetary bodies (Mars, Vesta, Moon) suggested that the C isotope composition of the bulk Earth is ~ -20‰ (Grady and Wright 2003; Grady et al. 1997). To infer the possibility that this composition could be different from that of the bulk Earth, one needs to assume that observed volatile depletion in C in the Earth does not yield any isotope fractionation. There has been a few experimental determinations of C isotope fractionation between C and iron carbide (Fe_3C, Reutsky et al. 2008; Satish-Kumar et al. 2011) or Fe-C molten alloy (Satish-Kumar et al. 2011) thought to represent metallic melt forming the core. The magnitude of this fractionation was confirmed by theoretical calculations by Horita and Polyakov (2015) who also concluded that the effect of pressure should be limited. It turns out that even at high temperatures, the isotope fractionation factor is relatively large, yielding a difference of up to 2-3‰ between carbon-bearing metallic melt and diamond (or carbonate) for T=2400-2800°C. A limitation of this calculation may be that the relevant species is the C dissolved in the silicate melt (e.g. Armstrong et al. 2015) rather than diamond. Wood et al. (2013) constructed a simple model to infer the $\delta^{13}C$ value of the mantle after core formation using existing data. By assuming a single stage model for core formation, they show that for reasonable temperatures of equilibration (T>2500 K), the isotope fractionation would be too small (2.4‰) compared with the observed difference between BSE and bulk Earth (15‰). As a result they called upon a Rayleigh distillation process corresponding to repeated episodes of equilibration during Earth accretion at weakly constrained temperatures of equilibration between 1500-1900 K. These seemed too low compared with what has been

inferred based on siderophile element partitioning, which implies a lack of constraints on the exact process that led to the observed carbon isotope fractionation.

4.2 Nitrogen isotopes

Nitrogen is another light element of interest in the context of the core formation. First, the N content of the BSE seems lower than chondritic and more depleted than other volatiles such as C, leading to a non-chondritic C/N of the Bulk Silicate Earth (Marty, 2012). This depletion may reflect large-scale metal-silicate equilibration during core formation, a massive blow-off of the early atmosphere or finally a consequence of the nature of the material accreted as a late veneer. Surprisingly, the partitioning of nitrogen was poorly characterized until recently. Now, it has been the focus of several studies aiming at determining its speciation (Roskosz et al. 2006b; Mysen et al.; 2010, Li et al., 2016) and its partitioning between metallic alloys, silicates and fluids at elevated pressures (Roskosz et al., 2013, Kadik et al., 2015; Li et al., 2016, Dalou et al., 2017). All these studies concluded that nitrogen was less siderophile than what would be anticipated from partitioning data at ambient pressure. Above an oxygen fugacity of IW-2.2, nitrogen is moderately siderophile. Furthermore, in more reducing conditions (below IW-2.2, the oxygen fugacity inferred for that of core-mantle equilibration on Earth), nitrogen may even become a lithophile element (Roskosz et al., 2013, Dalou et al., 2017). Yet, in any case, a significant fraction of nitrogen accreted on Earth may have been scavenged into the core forming alloys and the Earth's core is a major sink for nitrogen at the planetary scale. Consequently, if significant isotope fractionation occurred during metal-silicate equilibration, then the mantle and atmospheric N isotope compositions may have been modified relative to the pristine signature of the elusive bluiding blocks of the planet.

To date only one experimental dataset has been published on this topic (Li et al., 2016). Experiments were performed in both piston cylinder and multianvil apparatus at 1.5 and 7 GPa, and temperatures ranging from 1600 to 1800°C. In all experiments, a significant metal-silicate isotope fractionation was measured. The metal was on average found to be 3.5±1.7‰ lighter in ^{15}N than the silicate reservoir. No temperature dependence between 1600 and 1800°C was found, whereas the fractionation factors should decrease as a function of $1/T^2$. However, the uncertainties in the isotope fractionation factors (typically 2.5‰) may preclude the resolution of this effect. The authors proposed that this temperature effect could be counterbalanced by a positive pressure effect, however, such a large pressure effect has never been predicted or observed at such moderate pressures. These results should obviously be confirmed by future

experimental studies. Nonetheless, assuming that at least the order of magnitude and the direction of the fractionation are real, then this would imply that the average isotopic composition of the main carrier of nitrogen should be lighter by several ‰ than the BSE signature. In this context, only materials sharing isotopic similarities with the enstatite chondrites may be good candidates because carbonaceous chondrites exhibit a significant excess in ^{15}N (Marty et al., 2012; Li et al., 2016).

4.3 Silicon isotopes

There is considerable controversy regarding the silicon isotope fractionation between metal and silicate and its application to understanding core formation. First, an early study has shown that there is a measurable difference between the silicon isotope composition of chondrites and that of the bulk silicate Earth (Georg et al. 2007). It was argued that this isotope difference of 0.2‰ could be accounted for by the incorporation of Si in the core of the Earth and that assuming 7% Si in the core, the temperature of metal-silicate fractionation was approximately 2000 K. The temperature estimate was based on an *ab initio* calculation of Si isotope fractionation between Fe_3Si and Mg_2SiO_4 and it is clear that this was an estimate based on an approximate solid composition of liquid Fe-Ni-Si alloy and silicate melt. The temperature of metal-silicate equilibration was remarkably low and was therefore not realistic if one confronts this information with temperatures derived from siderophile element modeling (e.g. Wade and Wood 2005; Badro et al. 2007; ,Siebert et al. 2011; Rubie et al. 2011, Fisher et al. 2015) or with terrestrial magma ocean temperatures. A subsequent study by Fitoussi et al. (2009) showed that the difference between the Earth and carbonaceous chondrites was perhaps as low as 0.1‰ in which case the metal-silicate equilibration temperature could be as high as 2500 to 3000°C. The measurements of carbonaceous chondrites turned out to be difficult and did not yield consistent results with values ranging from -0.75‰ (Ziegler et al. 2010) to -0.36 ‰ (Armytage et al. 2011). As some of this scatter may be analytical, it seems difficult to determine precisely what the isotope composition of Si in the bulk Earth ought to be (Figure 5) based on chondrites.

Furthermore, as summarized in Hin et al. (2014) it seems difficult to infer precise temperatures of core formation, assuming a given Si content in the Earth's core using existing Si isotope fractionation factors between metal and silicate reported in the literature. This is due to the significant discrepancy between the data reported by the UCLA group (Shahar et al. 2009; 2011) and the data of Hin et al. (2014). The reason for this discrepancy is unresolved but it could be noted that the Si isotope data obtained by laser ablation in metals were not checked with a secondary standard and matrix effects in metals are undetermined. Similarly, data for Si

isotope fractionation in meteorites (Ziegler et al. 2010) is probably not an unambiguous method to assess the equilibrium isotope fractionation factor as there is no independent method to determine unequivocally whether the Si isotopes in these particular silicate and metallic phases were in isotope equilibrium, the diffusion of Si being notably slow in silicates. Thus, the debate is currently unsettled and needs additional experimental or theoretical data. Finally, an alternative view is that the Si isotope data would not be explained entirely by the effect of core formation but by the effect of vapor-condensate reactions in the protoplanetary disk (Fitoussi et al. 2009; Dauphas et al. 2015), by impact vaporization during accretion of planetesimals (Pringle et al 2014) or during giant impacts (Zambardi et al. 2013), or by volatilization from magma pools/oceans on planetesimals (Hin et al. 2017). In this case, the Si isotope signature of the bulk silicate Earth would only be partly affected by Si incorporation into the Earth's core.

4.4 Chromium isotopes

Chromium is a refractory metal that is siderophile only under reducing conditions. There has been clear documentation of strong isotope fractionation between the +III and +VI oxidation state of chromium in surface environments (e.g. Ellis et al. 2002) so it was logical to look at Cr isotopes as a tracer of metal-silicate fractionation. The first measurements of Cr isotopes in terrestrial rocks were reported by Schoenberg et al. (2008) and yielded a δ^{53}Cr value for BSE=-0.12±0.10‰. A study by Moynier et al. (2011) has shown a difference of up to +0.4‰ between the Cr isotope composition in terrestrial rocks and chondrites, which was interpreted as reflecting isotope fractionation taking place during core formation. The calculated temperature of metal-silicate equilibration was surprisingly low <1500 K, which was interpreted to reflect fractionation in small planetary bodies. This temperature was calculated using Cr isotope fractionation factor determined by *ab initio* calculations. Subsequent studies by Bonnand et al. (2016) and Schoenberg et al. (2016) showed that carbonaceous, ordinary and enstatite chondrites had δ^{53}Cr values of -0.111±0.065‰, -0.118±0.029‰ and -0.076±0.078‰ (Figure 6). Thus, these new studies show no Cr isotope difference between terrestrial rocks and chondrites, a result which contradicts the conclusions of Moynier et al. (2011). The origin for the discrepancy is unknown but it should be mentioned that the analytical technique used in both sets of studies differed. Bonnand et al (2016) and Schoenberg et al. (2016) used a double spike approach, while Moynier et al. (2011) did their measurements using a standard bracketting technique, which is more susceptible to analytical artefacts. Another point of interest is that Bonnand et al. (2016) also reported metal-silicate experiments used to determine the isotope fractionation factor of Cr between metal and silicate at 1650°C. The predictions of

Moynier et al. (2011) at this temperature for the equilibrium fractionation factor between an iron-chromium alloy ($Fe_{15}Cr$) and a Cr bearing olivine (e.g. $MgCr_2O_4$) agrees well with the average fractionation of <0.045‰ reported by Bonnand et al. (2016). Schauble et al. (2004) presented *ab initio* results for Cr-metal and Cr_2O_3, which differ by around 0.1‰ at 1500°C, but this is probably due to a larger differences in coordination and oxidation states. An additional complexity stems from the fact that Cr^{2+} is likely to be the species of Cr in the silicate melt rather than Cr^{3+} (Berry et al. 2006) which means that the fractionation factor would be even smaller. Altogether, there is currently little evidence that Cr isotopes in the Earth reflect a core signature due to the high temperature of core formation and the small magnitude of its isotopic fractionation.

4.5 Iron isotopes

The development of iron isotopes as a tool to study planetary differentiation has triggered a series of studies to investigate whether the formation of metallic cores could induce a measurable isotope fractionation. The first approach was to look for a difference between the iron isotope composition of chondrites and that of the silicate portion of the Earth. It was found that it was difficult to ascertain whether there is a resolvable difference in Fe isotopes between them or not (Poitrasson et al., 2004; Weyer et al., 2005; Schoenberg and von Blanckenburg, 2006; Williams et al., 2006; Craddock and Dauphas, 2011). The Fe isotope composition of basalts and peridotite xenoliths was found to be offset from that of chondrites by approximately 0.1‰ (Schoenberg and von Blanckenburg, 2006; Craddock et al. 2013; Teng et al. 2013). In contrast, Craddock et al. (2013) reported that abyssal peridotites (that are arguably depleted) have Fe isotope compositions similar to chondrites while Sossi et al. (2016) compiled all peridotite data and showed that fertile mantle appears to be resolvably heavier than chondrites, though significant scatter is still present. Since the Fe isotope fractionation during melting is not fully accounted for, it is a question whether any of the above mentioned samples is fully representative of the bulk Earth.

In parallel, a series of experimental and theoretical studies aimed at determining the isotope fractionation of iron between metal and silicate (Polyakov 2007; Polyakov and Mineev 2000; Poitrasson et al. 2009; Hin et al. 2012; Shahar et al. 2015; 2016). Here the results are again contrasted. Based on their experiments, Poitrasson et al. (2009) and Hin et al. (2012) concluded that there was no resolvable isotope fractionation between metal and silicate at temperatures that are relevant for the Earth's core formation. The experiments by Hin et al. (2012) were designed to investigate particularly low temperature (1250°C) to maximize the measured

isotope fractionation. To reach this goal, the experimental starting materials were doped with Sn so as to lower the melting point of the metallic alloy. One disadvantage was that it has been argued that the presence of Sn could modify the isotope fractionation factor (Young et al. 2015). This effect could indeed take place. However, Hin et al. (2012) showed that a tin-free and 30 wt% sulfur bearing experiment yielded exactly the same result within error. Poitrasson et al. (2009) had also found that the presence of 8 wt% did not change Fe isotope fractionation compared to a S-free system (Figure 7). These results were overall in agreement with the calculations of the beta factors from NRIXS measurements made by Polyakov et al. (2007) who predicted that iron metal (α-iron) should be heavier by 0.008‰ than FeO at 1250°C and 0.0075‰ at 1300°C which are the temperatures of the Hin et al. experiments.

More recently, however, Shahar et al. (2015) found a linear increase of the Fe isotope fractionation factor when increasing S contents from 0 to 17 wt% (Figure 7). Shahar et al. (2015) explained the difference between their observations and the previous studies of S-bearing systems by arguing that metal with 30 wt% S closely resembles sulphide and may therefore not be comparable to the inter-atomic bonding in the S-bearing metal of their study. In contrast with Shahar et al. (2015), an extensive study NRIXS of Liu et al. (2017) again found no significant difference in iron isotope fractionation between pure iron metal and iron alloyed with ~16 wt% S at all pressures (Figure 7). In fact, they could not resolve any significant effect of the alloying elements (H, C, O, Si, Ni, Si, S) present in the metallic phase larger than 0.02‰. In this context, the results of Elardo and Shahar (2017) pointing out an unexpected effect of the Ni content in metal on the partitioning of Fe isotopes between Fe-alloys and molten silicates certainly need to be critically evaluated and experimentally or spectroscopically confirmed.

Either way, the observations described above highlight the need for more thorough investigations into compositional effects on mass-dependent isotope fractionation between metal and silicate, as well as highlighting the need for a better understanding of how bonding environments in metallic alloys affect their isotopic compositions (see Young et al., 2015, on the effect of the bonding environments on the isotope compositions in silicates and oxides). If the Earth's Fe isotope composition is indeed enriched in heavy isotopes relative to that of chondrites, it is difficult to produce by core formation because experimental and NRIXS evidence imply that the Fe isotope fractionation between metal and silicate mantle should be either (i) negligible (Hin et al. 2014; Poitrasson et al. 2009, Liu et al. 2017) or (ii) reversed (Shahar et al. 2015; Elardo and Shahar 2017) and hence other processes possibly involving the volatility of Fe may be required (e.g. Poitrasson et al., 2004).

4.6 Nickel isotopes

As nickel is a major component of planetary cores, it seemed worth exploring the possibility of Ni isotope fractionation between metal and silicates. Lazar et al. (2012) have performed comprehensive experiments to determine the isotope fractionation factor between a Fe-Ni alloy and talc. While nickel talc ($Ni_3Si_4O_{10}(OH)_2$) does not represent the bulk composition of planetary mantle, it was a practical mineral for the experiments as talc can readily be separated from metal and is easily synthesized. Lazar et al. (2012) performed three-isotope experiments (see discussion above) to determine the metal-talc isotope fractionation factor for Ni. The experiments were performed in a piston cylinder to obtain temperatures ranging between 500°C and 900°C inside gold capsules for durations between 1 and 4000 minutes. There were several issues in these experiments including the loss of Ni to the Au container, inducing kinetic isotope fractionation during the experiments. Despite this difficulty, the authors extracted an equilibrium isotope fractionation factor that is described with the following equation:

$$\Delta^{62}Ni_{metal\_talc} = \frac{0.25 \pm 0.02 \times 10^6}{T^2} \quad (22)$$

It is arguable that this system is a good representation of the liquid metal-liquid silicate system but it is currently the only existing data set. With this fractionation factor it is possible to predict that the difference between the bulk Earth and bulk Silicate Earth should be less than 0.04‰ assuming that the temperature of metal silicate fractionation should be greater than 2500K. While the application of Ni isotopes to the Earth may be of limited interest, it may find more applications for studying the differentiation of small bodies where the highest temperature reached during core formation/metal segregation was smaller than that of the Earth.

4.7 Cu isotopes: evidence for the presence of sulfur?

Another important potential application of metal isotopes for constraining core formation is the case of chalcophile elements. There is considerable debate about the exact content of S in the core (O'Neill 1991; Badro et al. 2007; Wood et al. 2014; Suer et al. 2017) and it has been difficult to determine directly the S content of the core since S is a volatile element whose abundance in the core depends on the abundance of other light elements. Instead, chalcophile elements provide an indirect means of determining the sulfur content of the core as the metal/sulfide-silicate partitioning of these elements depend strongly on the presence of S. For example, Wood et al. (2014) have shown that there is a reasonable volatility trend for

chalcophile elements when one considers the sulfide-silicate partition coefficient rather than the S-free metal-silicate partition coefficient. Similarly, the presence of S explains the terrestrial value for the Mo/W ratio (Wood et al. 2014). This was taken as evidence for the presence of a sulfide matte, as had been argued in the early work of O'Neill (1991). The case of copper is of particular interest since it does not lie on the trend defined by Wood et al. (2014) and hence its behavior remains enigmatic. Savage et al. (2015) have measured the copper isotope composition of various chondrites as well as numerous terrestrial rocks and derived a $\delta^{65}Cu$ value of +0.07±0.10‰ for the bulk silicate Earth. Liu et al. (2015) obtained a similar value of +0.06±0.20‰ for the bulk silicate Earth. Savage et al. (2015) used the Cu isotope composition of chondrites to determine a putative composition for the bulk Earth using mixtures of chondrites as in Fitoussi and Bourdon (2012) and obtained a value of $\delta^{65}Cu$=-0.19±0.10 ‰. This value was reasonably close to another estimate using a mixture of EL and EH chondrites, $\delta^{65}Cu$=-0.24±0.09 ‰. One issue in this approach is that Cu is also a moderately volatile element (50% condensation temperature of 1037 K; Lodders 2003). Hence, the bulk Earth composition may not be simply inferred from that of chondrites (see for example the case of Zn isotopes, Luck et al. 2005). While it is not the purpose of this review to establish the validity of this approach for refractory elements, it may be riskier for volatile elements as the process causing volatile depletion could lead to isotope fractionation.

In addition, Savage et al. (2015) also attempted to determine Cu isotope fractionation factors between metal and silicate on the one hand and sulfide and silicate on the other hand using experiments with duration ranging between 30 seconds and a few minutes. At 1650°C, their metal-silicate fractionation factor varied between 0.06±0.06‰ and 0.15±0.09‰. For the sulfide-silicate experiments, the calculated $\Delta^{66}Cu$ value ranged between -1 to -20‰ due to uncertainties in mass balance calculations. The observed $\delta^{65}Cu$ in the bulk silicate Earth is higher than that predicted assuming only the separation of metallic iron as $\Delta^{66}Cu_{metal\text{-}silicate}$ precludes large isotope effects. In contrast, the separation of even a limited amount of sulfide as a sulfide matte results in large effects on the $\delta^{66}Cu$ of the BSE. This model cannot be fully quantified as the value of $\Delta^{66}Cu_{sulfide\_silicate}$ remains too poorly calibrated but it illustrates the potential of this isotope tracer to investigate poorly known aspects of core formation.

4.8 Molybdenum isotopes

In contrast with Fe, Si, Cr and Cu, the siderophile character of Mo is more pronounced, hence it is expected based on mass balance constraints that the isotope fractionation of Mo

associated with metal segregation should be enhanced in the silicate mantle. In the case of Mo isotopes, the expected isotope fractionation should be smaller than the other elements in principle because the relative difference in mass should scale with $1/m_2$-$1/m_1$ (see equation 20). Thus, if we compare $^{57}Fe/^{54}Fe$ and $^{98}Mo/^{95}Mo$, the fractionation factor of Mo should be smaller by a factor of 3, assuming that the force constants are of the same order of magnitude. In the case of Mo, however, there is possibly a component of nuclear volume fractionation that can increase the magnitude of the mass-dependent fractionation factor. There has been considerable work in recent years to determine precisely the Mo isotope composition of mantle-derived rocks (Greber et al. 2015, Liang et al. 2017; Willbold and Elliott 2017) and the value of $\delta^{98}Mo$ is thought to range between -0.21±0.06‰ to -0.16±0.06‰ (Figure 8) according to these studies (recalculated relative to the NIST SRM 3134 Mo standard). One degree of complexity is that there seems to be a small level of isotope fractionation between basaltic rocks and peridotites, possibly indicating a role for sulfides. In contrast, positive $\delta^{98}Mo$ values were obtained on average for continental rocks (<0.15‰, Willbold and Elliott 2017). In parallel, Burkhardt et al. (2014) have determined the $\delta^{98}Mo$ value of chondrites and their mean value is equal to -0.16±0.02‰ (relative to the NIST SRM 3134 Mo standard). Owing to uncertainties in the $\delta^{98}Mo$ of the BSE, it is possible that there is a slight isotope fractionation between the Bulk Earth represented by chondrites and the bulk silicate Earth.

Hin et al. (2013) have determined the isotope fractionation factor between metal and silicate using high temperature experiments under various conditions. It turns out that there is a measurable silicate-metal isotope fractionation factor of 0.19±0.03 at 1400°C while it is only 0.12±0.02‰ at 1600°C, which is consistent with a temperature dependent isotope fractionation. One question that arises is the oxidation state of Mo in the silicate (+VI or +IV). The transition from Mo(+VI) to Mo(+IV) occurs near IW-1 for CMAS melts (Holzheid et al., 1994; O'Neill and Eggins 2002; Leitzke et al. 2017) and possibly at higher f_{O2} for Fe-bearing melts. As core formation in the Earth took place at an oxygen fugacity of IW-2.2, Mo should be mostly present as Mo^{4+}.The redox conditions of the experiments were controlled with ΔIW ranging between -1.8 and +0.5. Given that the isotope fractionation factor was constant, this suggests that the oxidation state was either not highly variable or that it did not affect the isotope fractionation. Although the results show that the metal phase is enriched in light isotopes relative to the silicate phase, the relatively high temperatures expected for metal-silicate (2500-3000°C) combined with the siderophile properties of Mo lead to a maximum $\Delta^{98}Mo$ value of 0.05‰ approximately. Willbold and Elliott (2017) estimated that the maximum value of the BSE would be -0.1‰

based on mass balance, which is currently barely resolvable from the chondritic mean with existing analytical techniques. The slight offset of the δ^{98}Mo value for BSE suggested by Greber et al. (2015) and Liang et al. (2017) to -0.21‰ relative to chondrites would indicate that the BSE would have an enrichment in light isotope that be related to the presence of sulfides during core formation (Liang et al. 2017). Alternatively, as argued by Willbold and Elliott (2017), the δ^{98}Mo value for BSE can be estimated based on the Moon composition (-0.05±0.03‰, Burkhardt et al. 2014), assuming that the BSE and Moon were isotopically equilibrated at the time of Moon formation. In this case, the BSE would be identical to the chondritic value, provided the lunar core formed at a temperature of 2070 K, based on the isotope fractionation factor obtained by Hin et al. (2013), corresponding to a metal silicate fractionation factor of -0.11‰. The conclusion would be that core formation on Earth has not caused significant Mo isotope fractionation.

5. Quantitative modelling of isotope fractionation during core formation

Most models interpreting the stable isotope compositions of elements relevant to understanding of core formation considered each isotope system separately. In the simplest situation, it is possible to interpret the observations using a single stage model for core formation, assuming a single value for the temperature of core formation. In this case, if the partition coefficient of the element can be estimated based on experimental data, it is possible to use equation (5) to calculate the effect of core formation on the final silicate portion of the planet. More sophisticated models have considered the effect of a two-stage accretion (Fitoussi et al. 2009; Savage et al. 2015) or of continuous accretion process with a range of temperature as described in Ziegler et al. (2010), Zambardi et al.(2013) or Hin et al. (2014).

In most cases, single stage models have been considered despite the fact that it has been known for some time that varying conditions of core formation (Wade and Wood 2005, Rubie et al. 2011, 2015, Siebert et al. 2011, Fischer et al. 2015, Righter et al. 2016) or of the nature of accreting material (Rubie et al. 2011; Schönbächler et al. 2010) need to be considered in the case of the Earth. For example, the models of Hin et al. (2014) considering a continuous accretion and a mean temperature of 2577 K correspond to a difference between the bulk Earth and Bulk silicate Earth for δ^{30}Si of 0.14‰, while a single stage model for the same temperature yields a difference equal to 0.10‰ for the same Si concentration in the core. These differences can be understood in a broader context as the isotope record of core formation is strongly

dependent on the history of accretion (Yu and Jacobsen 2012, Dauphas 2017). In this framework, the overall history is well recorded by the least siderophile elements whereas the more siderophile elements only record the last part of accretion. When the partition coefficient is constant, it is possible to derive a simple form for the probability density function that an atom was delivered in the mantle at a given mass fraction of accreted Earth (Dauphas 2017). The situation is more complex when the partition coefficient is variable. Such is the case for silicon isotopes where the partition coefficient of Si depends highly on the oxygen fugacity as well as temperature and pressure. Thus, the larger Si isotope fractionation obtained with a continuous growth model reflects the fact the earlier part of accretion took place at lower temperatures, which in turn enhances isotope fractionation while the later part of accretion took place at higher temperatures with a higher metal-silicate partition coefficient.

To account for this complex behavior, we have implemented a new model derived from the general framework of Rudge et al. (2010) designed to describe the continuous chemical evolution of the mantle and core during accretion using mass balance equations. This model can take into account the variation of metal-silicate partition coefficients and also includes the possibility of incomplete equilibration between incoming metal and silicate mantle. This framework has been adapted to take into account the isotope fractionation taking place during metal-silicate fractionation. The mass fraction of accreted Earth is M(t) and it is a function of time. For the purpose of this study we have assumed a simple exponential function:

$$M(t) = M_O\left(1 - e^{-t/t_a}\right) \tag{23}$$

where M_0 is the final accreted mass fraction and t_a the accretion timescale. The fraction of metal accreted is F and it is assumed to be constant. The following basic equations were then solved for each isotope species separately:

$$\frac{dc_m^i}{dt} = \left[c_{me}^i + \frac{kF}{1-F} c_{ce}^i - \left(1 + \frac{kD_c^i(t)F}{1-F}\right) c_m^i \right] \frac{1}{M} \frac{dM}{dt} \tag{24}$$

$$\frac{dc_c^i}{dt} = \left[kD_c^i(t) c_m^i + (1-k) c_{ce}^i - c_c^i \right] \frac{1}{M} \frac{dM}{dt} \tag{25}$$

D_c^i represents the metal silicate partition coefficient for isotope i, k is a parameter describing degree of equilibration (k=1 being full equilibrium) c_{ce}^i, c_{me}^i, c_c^i and c_m^i representing the concentration of isotope i in the core and mantle of embryo, and in the core and mantle of the accreting planet, respectively. The variation of an isotope ratio can be written with the following equation:

$$\frac{dr_m}{dt} = \frac{d\left(c_m^2 / c_m^1\right)}{dt} = \frac{1}{c_m^1}\frac{dc_m^2}{dt} - \frac{c_m^2}{\left(c_m^1\right)^2}\frac{dc_m^1}{dt} \quad (26)$$

where r_m designates the isotope ratios in the mantle. If one considers equations (24-25) for two isotopes, it is possible to combine these equations into a single equation giving the variations of isotope ratios as a function of time in a more compact form:

$$\frac{dr_c}{dt} = (1-k)\frac{c_{ce}^1}{c_c^1}\left(r_{ce} - r_c\right)\frac{1}{M}\frac{dM}{dt} \quad (27)$$

$$\frac{dr_m}{dt} = \left[(1-k)\frac{c_{me}^1}{c_m^1}\left(r_{me} - r_m\right) + \frac{kF}{1-F}\frac{c_{ce}^1}{c_m^1}\left(r_{ce} - r_m\right) + r_m D\left(1-\alpha_{21}\right)\right]\frac{1}{M}\frac{dM}{dt} \quad (28)$$

where r_m and r_c designate the isotope ratios in the mantle and the core and with α_{ij} given by:

$$\alpha_{ij} = \frac{D_c^i}{D_c^j} = \frac{c_c^i}{c_c^j} \Big/ \frac{c_m^i}{c_m^j} \quad (29)$$

This equation is equivalent to equation (2) which is the definition of the equilibrium fractionation factor between metal and silicate. The equations written above have the advantage of being integrated numerically more readily than equations (24-25). The equations were also modified to take into account that the metal does not necessarily equilibrate with the entire silicate fraction upon accretion. This effect has been parameterized by Deguen et al. (2014) who showed that the parameter *k* could be replaced by a parameter k'=k/(1+D/Δm), where *Δm* represents the mass fraction of silicate equilibrated relative to the mass of the incoming metal. In this context, the value of *k* depends on the elements, which means that highly siderophile element (D>>1) are strongly influenced by the value of k, whereas less siderophile elements (D<1) such as Si or Cr are less affected. The value of the metal-silicate partition coefficients for each chemical species (i.e. Si and Cr) can be parameterized using the approach of Rudge et al. (2010) for an isotope *i* (the value for isotope *j* is rescaled from isotope *i*) using the equation:

$$\log_{10} D = a + b\frac{1}{T} + c\frac{P}{T} + dN - \frac{v}{4}\Delta IW - \frac{T_0}{T}\log_{10}\gamma_M^{met}(T_0) + \frac{v}{2}\log_{10}\gamma_{FeO}^{sil} \quad (30)$$

where T is the temperature in K, P the pressure in GPa, v the valence, N the molar ratio of non bridging oxygens to tetrahedral cations in the silicate melt, T_0 =1873 K, and γ_M^{met} and γ_{FeO}^{silmet} are the activity coefficients of element M in the metal and the activity coefficient of FeO in the silicate, and a-d are empirical regression parameters. The temperature is assumed to be a function of the pressure of equilibration which is taken as the liquidus pressure and the following equation was used as in Rudge et al. (2010):

$$T = 1973 + 28.57P \quad (31)$$

The pressure of metal-silicate equilibration is then assumed to increase as the planet grows with the following function:

$$P = P_0\left(1 - e^{-t/\tau}\right)^{\frac{2}{3}} \quad (32)$$

where P_0 is a fixed value. The set of four ordinary differential equations (27-28, two for each isotope) corresponding to the metal and silicate phase were solved numerically using the Matlab™ software. For the case of molybdenum, the parameterization of the metal-silicate partition coefficient given in Righter et al. (2010) was used, with a bulk silicate Earth composition taken from Rubie et al. (2011). In this model we have tried to reproduce the P, T and f_{O2} conditions of core formation in the models of Fischer et al. (2015) and Rudge et al. (2010) with variable f_{O2}. It was assumed that the oxygen fugacity increases starting from an initial value IW_1, with the following dependence on t:

$$IW(t) = IW_1 + \Delta IW \times \left(1 - e^{-t/\tau}\right)^n \quad (33)$$

where ΔIW=1.5 and n=3. The results of the models are plotted in Figures 9-13. For Si and Cr, a decrease in oxygen fugacity corresponds to a greater fraction of Si or Cr partitioned into the metal phase and this leads to a greater isotope fractionation in the silicate phase (Figures 9 and 10). Such an effect would also be predicted from equation (5). This effect is also seen for Mo which is always strongly partitioned into the liquid metal especially at low oxygen fugacities (Figure 11). As the metal-silicate partition coefficient for Si increases with increasing P and T, the isotope fractionation in the silicate also increases due to increasing partitioning of Si in the metal compensating the decrease in isotope fractionation factor with T (Figure 9). The reverse effect is observed for Cr as the metal-silicate partition coefficient decreases as accretion proceeds (e.g. Corgne et al. 2008). The model predicts that under similar T, P f_{O2} conditions, the Si isotope fractionation between the bulk silicate Earth and the bulk Earth is measurable while that for Cr and Mo cannot be resolved, which is overall consistent with the existing data (see discussion above). In detail, the best fit is obtained for a starting f_{O2} (IW_1) equal to IW-3.5. This matches the Si, Cr and Mo isotope observations and is within the right order of magnitude for Si and Cr depletion in the Earth's mantle. The advantage of this model presented here is to be able to reach these conclusions with a common modelling approach.

This model also takes into account the effect of incomplete equilibration between metal and silicate corresponding to the extreme cases of core merging with no equilibration (k=0) and full equilibration (k=1). In this context, the conditions of core formation in the embryos play a role. The more contrasted the conditions are during embryo core formation relative to the case of the Earth, the more effect incomplete equilibration has on the final isotope composition in the

silicate Earth. To illustrate this, we have considered a case where core formation in the embryos took place at an oxygen fugacity of IW-3.5 (corresponding for example to reducing conditions as observed in aubrites or enstatite chondrites) with a fixed P and T of equilibration (5 GPa, 2115 K), while it followed an evolution from IW-3.5 to IW-1.5 in the accreting planet. As shown in Figure 12, for k=0.1, the Si isotope fractionation is minimal, as the isotope fractionation due to metal-silicate fractionation is smaller in embryos, due to low metal-silicate partition coefficient for Si in embryos. However, when equilibration is larger (k=0.9), the net Si isotope fractionation is greater because the larger incorporation of Si in the metal yields a large δ^{30}Si value in the silicate mantle. Finally, one can also examine the case of imperfect equilibration using the formalism developed by Deguen et al. (2014) who took into account the fact that the equilibration volume of the metal did not represent the whole mantle volume. As shown in Figure 13, for large values of Δm (100), the results for Si isotopes are identical to the case shown above in Figure 9b with initial oxygen fugacity IW-3.5. For smaller values of Δm, the equilibration is less extensive and this is equivalent to reducing the value of k, in which case the δ^{30}Si is lower, as explained above. Again, for low values of Δm, the conditions of core formation in the embryos become more predominant.

In summary, these model results are overall consistent with the observations for Si, Cr and Mo in the Earth. The limited isotope fractionation observed for Cr cannot be explained by low T of core formation in embryos, if we explain the data jointly with the Si isotope data. The Mo isotope signature reflects the overall high temperature of core formation in the Earth and the Si isotopes could reflect low temperature of core formation in embryos but this would require little equilibration (k small) in contrast with the conclusions of Rudge et al. (2010). As shown above, low oxygen fugacity (IW-3.5) during the initial stages of accretion followed by more oxidizing conditions (IW-1.5) can explain the Si isotope observations, while matching the siderophile element data (e.g. Fischer et al. 2015) and the Mo and Cr isotope observations. More systematic exploration of the parameter space would be useful but is beyond the scope of this review. Altogether this modelling approach provides a useful means of testing the key parameters controlling the isotope fractionation of metals incorporated into the core, while including the most up to date processes.

7. Conclusions

Constraining the conditions of core formation in planets has become a key target for understanding the accretion process and the early evolution of planets. The development of new isotope tools that could provide new views on these processes is thus most welcome. As

outlined in this review, the magnitude of isotope fractionation between metal and silicate at the temperature of Earth core formation is small, which limits the applicability of these systems to understand the formation of the Earth's core. If anything, the isotope data confirm that the core-metal separation took place at temperature >2500 K. Current analytical methods do not always allow a resolution of these isotope effects. An increase in analytical precision and a better characterization of the isotope fractionation factors would be desirable to extend the applications of this method. There is, however, a scope in applying these tools to planets or planetesimals where the temperature of metal-silicate separation was smaller. For the case of volatile elements, one must first constrain the bulk isotope composition of the planet which is a difficult problem to tackle but the examination of achondrite bodies with volatile element depletion or of lithophile elements with similar volatility may offer a solution. There are still clear gaps in being able to fully use these tools in particular since the isotope fractionation factors are not always available. With increasingly more precise measurements, this approach for constraining core formation will certainly provide important clues in the future.

Acknowledgements: We thank Paolo Sossi and one anonymous reviewer for their comments that greatly helped improve the manuscript.

References

Armstrong, L.S., Hirschmann, M.M., Stanley, B.D., Falksen, E.G., Jacobsen, S.D., 2015. Speciation and solubility of reduced C–O–H–N volatiles in mafic melt: Implications for volcanism, atmospheric evolution, and deep volatile cycles in the terrestrial planets, Geochim. Cosmochim. Acta 171, 283–302.

Armytage, R.M.G., Georg, R.B., Savage, P.S., Williams, H.M., Halliday, A.N., 2011. Silicon isotopes in meteorites and planetary core formation. Geochim. Cosmochim. Acta 75, 3662-3676.

Badro, J., Fiquet, G., Guyot, F., Gregoryanz, E., Occelli, F., Antonangeli, D., d'Astuto, M., 2007. Effect of light elements on the sound velocities in solid iron: Implications for the composition of Earth's core. Earth Planet. Sci. Lett. 254, 233-238.

Berry, A.J., O'Neill, H.S.C., Scott, D.R., Foran, G.J., Shelley J.M.G., 2006. The effect of composition on Cr^{2+}/Cr^{3+} in silicate melts, Am. Min. 91, 1901-1908.

Bigeleisen J. and Mayer M. G., 1947. Calculation of equilibrium constants for isotopic exchange reactions. J. Chemical Physics 15, 261-267.

Blanchard, M., Dauphas, N., Hu, M.Y., Roskosz M., Alp, E.E., Golden, D.C., Sio, C.K., Tissot F.L.H., Zhao, J., Gao, L., Morris, R.V., Fornace, M., Floris, A., Lazzeri M., Balan, E., 2015. Reduced partition function ratios of iron and oxygen in goethite, Geochim. Cosmochim. Acta 151, 19-33.

Bonnand, P., Williams, H.M., Parkinson, I.J., Wood, B.J., Halliday A.N. (2016) Stable chromium isotopic composition of meteorites and metal–silicate experiments: Implications for fractionation during core formation, Earth Planet. Sci. Lett. 435, 14-21.

Brenan, J.M., 2008. Re-Os fractionation by sulfide melt-silicate melt partitioning: A new spin. Chem. Geol. 248, 140-165.

Burkhardt, C., Hin, R.C., Kleine, T., Bourdon B., 2014. Evidence for Mo isotope fractionation in the solar nebula and during planetary differentiation, Earth Planet. Sci. Lett. 391, 201-211.

Cao, X., Bao, H., 2017. Redefining the utility of the three-isotope method, Geochim. Cosmochim. Acta, 212, 16-32.

Canup, R.M., 2008. Accretion of the Earth, Philosophical Transactions of the Royal Society A: Mathematical, Physical and Engineering Sciences, 366, 4061-4075.

Charlier, B.L.A., Ginibre, C., Morgan, D., Nowell, G.M., Pearson, D.G., Davidson, J.P., Ottley, C.J., 2006. Methods for the microsampling and high-precision analysis of strontium and rubidium isotopes at single crystal scale for petrological and geochronological applications. Chem. Geol. 232, 114-133.

Chakrabarti, R., Jacobsen, S.B., 2010. Silicon isotopes in the inner Solar System: Implications for core formation, solar nebular processes and partial melting. Geochim. Cosmochim. Acta 74, 6921-6933.

Chou, I.-M., 1987. Oxygen buffer and hydrogen sensor techniques at elevated pressures and temperatures, in Hydrothermal Experimental Techniques, edited by G. C. Ulmer and H. C. Barnes, John Wiley, New York pp. 60 – 99.

Cohen, B.A., Levasseur, S., Zanda, B., Hewins, R.H., Halliday, A.N., 2006. Kinetic isotope effect during reduction of iron from a silicate melt. Geochim. Cosmochim. Acta 70, 45.

Cole, D.R., Ohmoto, H., Lasaga, A.C., 1983. Isotopic exchange in mineral-fluid systems. I. Theoretical evaluation of oxygen isotopic exchange accompanying surface reactions and diffusion, Geochim. Cosmochim. Acta, 47, 1681-1693.

Corgne, A., Keshav, S., Wood, B.J., McDonough, W.F. Fei, Y. 2008. Metal–silicate partitioning and constraints on core composition and oxygen fugacity during Earth accretion, Geochim. Cosmochim. Acta 72, 574–589.

Craddock, P.R., Dauphas, N., 2011. Iron isotopic composition of reference materials, geostandards and chondrites. Geostand. Geoanal. Res. 35, 101-123.

Craddock, P.R., Warren, J.M, Dauphas, N., 2013. Abyssal peridotites reveal the near-chondritic Fe isotopic composition of the Earth, Earth Planet. Sci. Lett. 365, 63-76.

Criss, R.E., Gregory, R.T., Taylor, H.P., 1987. Kinetic theory of oxygen isotopic exchange between minerals and water. Geochim. Cosmochim. Acta 51, 1099-1108.

Dahl, T.W., Stevenson, D.J., 2010. Turbulent mixing of metal and silicate during planet accretion—and interpretation of the Hf–W chronometer, Earth Planet. Sci. Lett. 295, 177-186.

Dalou, C., Hirschmann, M.M., von der Handt, A., Mosenfelder, J., Armstrong, L.S., 2017. Nitrogen and carbon fractionation during core–mantle differentiation at shallow depth, Earth Planet. Sci. Lett. 458, 141-151.

Dauphas N., 2017. The isotopic nature of the Earth's accreting material through time, Nature 541, 521-524.

Dauphas, N., Roskosz, M., Alp, E.E., Golden, D.C., Sio, C.K., Tissot, F.L.H., Hu, M.Y., Zhao, J., Gao, L., Morris, R.V., 2012. A general moment NRIXS approach to the determination of equilibrium Fe isotopic fractionation factors: application to goethite and jarosite, Geochim. Cosmochim. Acta 94, 254-275

Dauphas, N., Roskosz M., Alp E.E., Neuville D.R., Hu M.Y., Sio C.K., Tissot, F.L.H., Zhao, J., Tissandier, L., Médard, E., Cordier, C., 2014. Magma redox and structural controls on iron isotope variations in Earth's mantle and crust, Earth Planet. Sci. Lett. 398, 127-140.

Dauphas, N., Poitrasson, F., Burkhardt, C., Kobayashi, H., Kurosawa, K., 2015. Planetary and meteoritic Mg/Si and δ^{30}Si variations inherited from solar nebula chemistry. Earth Planet. Sci. Lett. 427, 236-248.

Deguen, R. Landeau, M. Olson M. 2014. Turbulent metal–silicate mixing, fragmentation, and equilibration in magma oceans, Earth Planet. Sci. Lett., 391, 274-287.

Drake, M.J., Newsom, H. E. Capobianco, C. J., 1989. V, Cr, and Mn in the Earth, Moon, EPB, and SPB and the origin of the Moon: Experimental studies, Geochim. Cosmochim. Acta, 53, 2101-2111.

Edgar A.D., 1973. Experimental Petrology. Basic principles and techniques. Clarendon Press, Oxford, 217 pp.

Elardo, S.M., Shahar, A., 2017. Non-chondritic iron isotope ratios in planetary mantles as a result of core formation, Nature Geosci. 10, 317-321.

Ellis, A.S., Johnson, T.M., Bullen, T.D., 2002. Cr isotopes and the fate of hexavalent chromium in the environment. Science 295, 2060–2062.

Ellison, A.J., Hess, P.C., 1986. Solution behavior of +4 cations in high silica melts - Petrologic and geochemical implications. Contrib. Mineral. Petrol. 94, 343-351.

Eugster H.P., 1957. Heterogeneous reactions involving oxidation and reduction at high temperatures and pressures, J. Chem. Phys. 26, 1760-1761.

Fischer, R.A., Nakajima, Y., Campbell, A.J., Frost, D.J., Harries, D., Langenhorst, F., Miyajima, N., Pollok, K., Rubie, D.C., 2015. High pressure metal-silicate partitioning of Ni, Co, V, Cr, Si, and O. Geochim. Cosmochim. Acta 167, 177–194.

Fitoussi C., Bourdon B., Kleine T., Oberli F., and Reynolds B. C., 2009. Si isotope systematics of meteorites and terrestrial peridotites: implications for Mg/Si fractionation in the solar nebula and for Si in the Earth's core. Earth Planet. Sci. Lett. 287, 77-85.

Fitoussi, C., Bourdon, B., 2012. Silicon isotope evidence against an enstatite chondrite Earth, Science 335, 1477-1480.

Georg R. B., Halliday A. N., Schauble E. A., and Reynolds B. C., 2007. Silicon in the Earth's core. Nature 447, 1102-1106.

Grady, M.M., Wright, I.P. 2003. Elemental and isotopic abundances of carbon and nitrogen in meteorites. Space Sci Rev 106, 231-248

Grady, M.M., Wright I.P., Pillinger C.T., 1997. Carbon in howardite, eucrite and diogenite basaltic achondrites Meteor. Planet. Sci. 32,863-868

Greber, N. D. Puchtel, I. S. Nägler, T.F., Mezger, K., 2015. Komatiites constrain molybdenum isotope composition of the Earth's mantle, Earth Planet. Sci. Lett. 421,129–138.

Gupta, C.P., Lal, K.C., 1972 Temperature Shift, recoil-free fraction, and force constant in Mossbauer Studies, in Temperature Shift in Mossbauer Studies 51, 233-239.

Halliday, A. N., 2004. Mixing, volatile loss and compositional change during impact-driven accretion of the Earth, Nature 427, 505-509.

Hillgren, V.J., Drake, M.J., Rubie, D.C., 1996. High pressure and high temperature metal-silicate partitioning of siderophile elements: The importance of silicate liquid composition. Geochim. Cosmochim. Acta 60, 2257-2263.

Hin, R.C., Burkhardt, C., Schmidt, M.W., Bourdon, B., Kleine, T., 2013. Experimental evidence for Mo isotope fractionation between metal and silicate liquids. Earth Planet. Sci. Lett. 379, 38-48.

Hin, R.C., Fitoussi, C., Schmidt, M.W., Bourdon, B., 2014. Experimental determination of the Si isotope fractionation factor between liquid metal and liquid silicate. Earth Planet. Sci. Lett. 387, 55-66.

Hin, R.C., Schmidt, M.W., Bourdon, B., 2012. Experimental evidence for the absence of iron isotope fractionation between metal and silicate liquids at 1 GPa and 1250–1300 °C and its cosmochemical consequences. Geochim. Cosmochim. Acta 93, 164-181.

Hin R. C., Coath C. D., Carter P. J., Nimmo F., Lai Y.-J., Pogge von Strandmann P. A. E., Willbold M., Leinhardt Z. M., Walter M. J. & Elliott T. 2017. Magnesium isotope evidence that accretional vapour loss shapes planetary compositions, Nature 549, 511–515.

Holzheid, A., Borisov, A., Palme H., 1994. The effect of oxygen fugacity and temperature on solubilities of nickel, cobalt, and molybdenum in silicate melts Geochimica et Cosmochimica Acta 58, 1975-1981.

Horita, J., Polyakov, V.B., 2015. Carbon-bearing iron phases and the carbon isotope composition of the deep Earth, Proc. Nat. Acad. Sci., 112, 31-36.

Huebner J.S., 1987. Use of gas mixtures at low pressure to specify oxygen and other fugacities of furnace atmospheres. In: Ulmer GC, Barnes HL (eds) Hydrothermal experimental techniques. John Wiley and Sons, New York, pp 20-60.

Kadik, A. A., Koltashev, V. V., Kryukova, E. B., Plotnichenko, V. G., Tsekhonya, T. I., Kononkova, N.N., 2015. Solubility of nitrogen, carbon, and hydrogen in $FeO–Na_2O–Al_2O_3–SiO_2$ melt and liquid iron alloy: influence of oxygen fugacity, 9, Geochem. Int., 53, 849–868.

Kempl, J., Vroon, P.Z., Zinngrebe, E., van Westrenen, W., 2013. Si isotope fractionation between Si-poor metal and silicate melt at pressure–temperature conditions relevant to metal segregation in small planetary bodies, Earth Planet. Sci. Lett., 368, 61-68.

Kempl, J., Vroon, P.Z., van der Wagt, B., Zinngrebe, E., Frost, D.J., van Westrenen, W., 2016. Silicon stable isotope fractionation between metal and silicate at high-pressure, high-temperature conditions as a tracer of planetary core formation. Neth J Geosci 95, 113-129.

Kieffer, S.W., 1982. Thermodynamics and lattice vibrations of minerals: 5. applications to phase equilibria, isotopic fractionation, and high-pressure thermodynamic properties, Rev. Geophys. Space Phys. 20, 827-849.

Kohn V.G., Smirnov G.V., 1998.Theory of nuclear resonant scattering of synchrotron radiation in the presence of diffusive motion of nuclei. II.Phys. Rev. B 57, 5788-5797.

Kyser, T.K., Lesher, C.E., Walker, D., 1998. The effects of liquid immiscibility and thermal diffusion on oxygen isotopes in silicate liquids. Contrib. Mineral. Petrol. 133, 373-381.

Lazar, C., Young, E.D., Manning, C.E., 2012. Experimental determination of equilibrium nickel isotope fractionation between metal and silicate from 500 degrees C to 950 degrees C. Geochim. Cosmochim. Acta 86, 276-295.

Leitzke, F.P., Fonseca, R.O.C., Sprung, P., Mallmann, G., Lagos, M., Michely, L.T., Münker, C., 2017. Redox dependent behaviour of molybdenum during magmatic processes in the terrestrial and lunar mantle: Implications for the Mo/W of the bulk silicate Moon, Earth Planet. Sci. Lett., 474, 503-515.

Lesher, C.E., 1990. Decoupling of chemical and isotopic exchange during magma mixing. Nature 344, 235-237.

Li, Y.-F. Marty, B Shcheka S, Zimmermann L, Keppler H. 2016 Nitrogen isotope fractionation during terrestrial core-mantle separation. Geochem. Persp., 2, <10.7185/geochemlet.1614>.

Liang , Y.-H. Halliday A. N., Siebert C., Godfrey Fitton J., Burton K.W., Wang K.-L., Harvey J. 2017. Molybdenum isotope fractionation in the mantle, Geochim. Cosmochim. Acta 199, 91–111.

Lipkin, H.J. (1995) Mössbauer sum rules for use with synchrotron sources, Phys. Rev. B, 52, 10073-10079.

Liu, S.-A., Huang, J. Liu, J., Wörner, G., Yang, W., Tang, Y.-J., Chen, Y., Tang, L., Zheng, J., Li, S., 2015. Copper isotopic composition of the silicate Earth, Earth and Planetary Science Letters, 427, 95-103.

Liu, J., Dauphas, N., Roskosz, M., Hu, M.Y., Yang, H., Bi, W., Zhao, J., Alp, E.E., Hu J.Y., and Lin J.-F., 2017. Iron isotopic fractionation between silicate mantle and metallic core at high pressure, Nature Comm.

Lodders, K., 2003. Solar system abundances and condensation temperatures of the elements, Astrophys. J. 591, 1220-1247.

Lord, O.T., Walter, M.J., Dasgupta, R., Walker, D., Clark, S.M., 2009. Melting in the Fe-C system to 70 GPa. Earth Planet. Sci. Lett. 284, 157-167.

Luck, J.-M. Ben Othman, D., Albarède, F., 2005. Zn and Cu isotopic variations in chondrites and iron meteorites: Early solar nebula reservoirs and parent-body processes, Geochim. Cosmochim. Acta 69, 5351-5363.

Ma, Z.T., 2001. Thermodynamic description for concentrated metallic solutions using interaction parameters. Metall. Mater. Trans. B 32, 87-103.

Mann, U., Frost, D.J., Rubie, D.C., 2009. Evidence for high-pressure core-mantle differentiation from the metal–silicate partitioning of lithophile and weakly-siderophile elements, Geochim. Cosmochim. Acta, 73, 7360-7386.

Marty, B., 2012.The origins and concentrations of water, carbon, nitrogen and noble gases on Earth,Earth Planet. Sci. Lett., 313–314, 56-66.

Matjuschkin, V., Brooker, R.A., Tattitch, B., Blundy, J.D., Stamper, C.C. (2015) Control and monitoring of oxygen fugacity in piston cylinder experiments. *Contributions to Mineralogy and Petrology* 169, 9.

Matsuhisa, Y., Goldsmith, J.R., Clayton, R.N., 1978. Mechanisms of Hydrothermal Crystallization of Quartz at 250°C and 15 Kbar. Geochim. Cosmochim. Acta 42, 173-182.

Médard, E., Schmidt, M.W., Walle, M., Keller, N.S., Gunther, D., 2015. Platinum partitioning between metal and silicate melts: Core formation, late veneer and the nanonuggets issue. Geochim. Cosmochim. Acta 162, 183-201.

Milot, J., Poitrasson, F., Baron, S. Coustures M.-P. 2016. Iron isotopes as a potential tool for ancient iron metals tracing, J. Archaeol. Sci., 76, 9-20.

Moynier, F., Yin, Q.Z., Schauble, E., 2011. Isotopic evidence of Cr partitioning into Earth's core. Science 331, 1417-1420.

Mysen, B.O., Fogel M.L., 2010. Nitrogen and Hydrogen Isotope compositions and solubility in silicate melts in equilibrium with reduced (N + H)-bearing fluids at high pressure and temperature: effects of melt structure. Am. Mineral., 95, 987-999.

Mysen, B. O., Eggler, D. H., Seitz, M.G. and Holloway, J. R., 1976. Carbon dioxide in silicate melts and crystals. Part. I. Solubility measurements. Amer. J. Sci. 276, 455-479.

Northrop, D.A., Clayton, R.N., 1966. Oxygen-isotope fractionations in systems containing dolomite. J. Geol. 74, 174-196.

O'Neill H.St.C. 1991. The origin of the moon and the early history of the earth—A chemical model. Part 2: The Earth, Geochim. Cosmochim. Acta, 55, 1159-1172.

O'Neill, H.S.C., Canil, D., Rubie, D.C., 1998. Oxide-metal equilibria to 2500° C and 25 GPa: Implications for core formation and the light component in the Earth's core, J. Geophys. Res. (B) 103, 12239-12260.

O'Neill, H.S.C., Eggins S.M., 2002. The effect of melt composition on trace element partitioning: an experimental investigation of the activity coefficients of FeO, NiO, CoO, MoO_2 and MoO_3 in silicate melts Chem. Geol., 186, 151-181.

Poirier J.P., 1994. Light elements in the Earth's outer core: a critical review, Phys. Earth Planet. Interiors, 85, 319-337.

Poitrasson F., Roskosz M., and Corgne A., 2009. No iron isotope fractionation between molten alloys and silicate melt to 2000 degrees C and 7.7 GPa: Experimental evidence and implications for planetary differentiation and accretion. Earth Planet. Sci. Lett. 278, 376-385.

Poitrasson F., Halliday A. N., Lee D. C., Levasseur S., and Teutsch N., 2004. Iron isotope differences between Earth, Moon, Mars and Vesta as possible records of contrasted accretion mechanisms. Earth Planet. Sci. Lett. 223, 253-266.

Polyakov V. B. and Mineev S. D., 2000. The use of Mössbauer spectroscopy in stable isotope geochemistry. Geochim. Cosmochim. Acta 64, 849-865.

Polyakov V. B., Clayton R. N., Horita J., and Mineev S. D., 2007. Equilibrium iron isotope fractionation factors of minerals: Reevaluation from the data of nuclear inelastic resonant X-ray scattering and Mossbauer spectroscopy. Geochim. Cosmochim. Acta 71, 3833-3846.

Polyakov V. B., 2009. Equilibrium Iron Isotope Fractionation at Core-Mantle Boundary Conditions. Science 323, 912-914.

Pringle, E.A., Moynier, F., Savage, P.S., Badro, J., Barrat J.A., 2014. Silicon isotopes in angrites and volatile loss in planetesimals, Proc.Nat. Acad. Sci. 111, 17029-17032.

Qin, L., Xia, J., Carlson, R.W., Zhang, Q., 2015. Chromium stable isotope composition of meteorites. 46th Lunar Planet, Sci Conf.

Randl, G., Vogl, G., Petry, W., Hennion, B., Sepiol, B., Nembach, K., 1995. Lattice dynamics and related diffusion properties of intermetallics: I. Fe_3Si, J. Phys.: Condens. Matter 7, 5983-5999.

Reutsky, V. N., Borzdov, Y. M., Palyanov, Y. N., 2008. Carbon isotope fractionation associated with HPHT crystallization of diamond. Diamond Relat. Mater. 17,1986–1989.

Richter, F.M., Dauphas, N., Teng, F.Z., 2009. Non-traditional fractionation of non-traditional isotopes: Evaporation, chemical diffusion and Soret diffusion. Chem. Geol. 258, 92-103.

Richter, F.M., Watson, E.B., Mendybaev, R.A., Teng, F.Z., Janney, P.E., 2008. Magnesium isotope fractionation in silicate melts by chemical and thermal diffusion. Geochim. Cosmochim. Acta 72, 206-220.

Righter, K., Drake, M.J., 2000. Metal/silicate equilibrium in the early Earth-New constraints from the volatile moderately siderophile elements Ga, Cu, P, and Sn, Geochim. Cosmochim. Acta, 64, 3581-3597.

Righter, K., Pando, K.M., Danielson, L., Lee, C.-T., 2010. Partitioning of Mo, P and other siderophile elements (Cu, Ga, Sn, Ni, Co, Cr, Mn, V, and W) between metal and silicate melt as a function of temperature and silicate melt composition, Earth Planet. Sci. Lett. 291, 1-9.

Righter, K. Danielson L.R., Pando K.M., Shofner G.A., Sutton S.R., Newville M., Lee C.-T., 2016. Valence and metal/silicate partitioning of Mo: Implications for conditions of Earth accretion and core formation, Earth Planet. Sci. Lett. 437, 89–100.

Roeder, P.L., Dixon, J.M., 1977. Centrifuge Furnace for Separating Phases at High-Temperature in Experimental Petrology. Can. J. Earth Sci. 14, 1077-1084.

Roskosz, M., Bouhifd, M.A., Jephcoat, A.P., Marty, B., Mysen, B.O., 2013. Nitrogen solubility in molten metal and silicate at high pressure and temperature. Geochim. Cosmochim. Acta 121, 15-28.

Roskosz, M., Mysen, B.O., Cody, G.D., 2006b. Dal speciation of nitrogen in silicate melts at high pressure and temperature: An experimental study. Geochim. Cosmochim. Acta 70, 2902-2918.

Roskosz, M., Luais, B., Watson, H.C., Toplis, M.J., Alexander, C.M.O., Mysen, B.O., 2006. Experimental quantification of the fractionation of Fe isotopes during metal segregation from a silicate melt. Earth Planet. Sci. Lett. 248, 851-867.

Roskosz, M., Sio, C.K., Dauphas, N., Bi, W., Tissot, F.L.H., Hu, M.Y., Zhao, J., Alp, E.E. 2015. Spinel–olivine–pyroxene equilibrium iron isotopic fractionation and applications to natural peridotites, Geochim. Cosmochim. Acta 169, 184-199.

Rotaru, M., Birck, J.L., Allegre, C.J., 1992. Clues to Early Solar-System History from Chromium Isotopes in Carbonaceous Chondrites. Nature 358, 465-470.

Rubie, D. C., Frost, D. J., Mann, U., Asahara, Y., Nimmo, F., Tsuno, K., & Palme, H., 2011. Heterogeneous accretion, composition and core–mantle differentiation of the Earth. Earth Planet. Sci. Lett. 301(1), 31-42.

Rubie, D.C., Jacobson, S.B., Morbidelli, A., O'Brien, D.P., Young, E.D., de Vries, J., Nimmo, F., Palme, H., Frost, D.J. 2015. Accretion and differentiation of the terrestrial planets with implications for the compositions of early -formed Solar System bodies and accretion of water. Icarus 248, 89-108.

Rudge, J.F., Kleine, T., Bourdon, B., 2010. Broad bounds on Earth's accretion and core formation constrained by geochemical models Nature Geoscience 3, 439-443.

Satish-Kumar, M., So, H., Yoshino, T., Kato, M., Hiroi, Y., 2011. Experimental determination of carbon isotope fractionation between iron carbide melt and carbon: ^{12}C-enriched carbon in the Earth's core? Earth Planet. Sci. Lett. 310, 340-348.

Savage, P.S., Georg, R.B., Armytage, R.M.G., Williams, H.M., Halliday, A.N., 2010. Silicon isotope homogeneity in the mantle. Earth Planet. Sci. Lett. 295, 139-146.

Savage, P.S.,Moynier, F., 2013. Silicon isotopic variation in enstatitemeteorites: clues to their origin and Earth-forming material. Earth and Planetary Science Letters 361, 487–496.

Savage, P.S., Moynier, F., Chen H., Shofner, G., Siebert, J., Badro, J., Puchtel, I.S. 2015. Copper isotope evidence for large-scale sulphide fractionation during Earth's differentiation, Geochemical Perspectives Letters 1, 53-64.

Schauble E.A., 2004. Applying stable isotope fractionation theory to new systems. Rev Mineral Geochem 55, 65-111.

Schauble, E., Rossman, G.R., Taylor, H.P., 2004. Theoretical estimates of equilibrium chromium-isotope fractionations, Chem. Geol. 205, 99-114.

Schmidt, M.W., Connolly, J.A.D., Gunther, D., Bogaerts, M., 2006. Element partitioning: The role of melt structure and composition. Science 312, 1646-1650.

Schoenberg R. and von Blanckenburg F., 2006. Modes of planetary-scale Fe isotope fractionation. Earth Planet. Sci. Lett. 252, 342-359.

Schoenberg, R., Zink, S., Staubwasser, M., von Blanckenburg, F.; 2008. The stable Cr isotope inventory of solid Earth reservoirs determined by double-spike MC-ICP-MS. Chem. Geol. 249, 294-306.

Schoenberg, R., Merdian, A., Holmden. C., Kleinhanns, I.C., Hassler, K., Wille, M., Reitter, E., 2016. The stable Cr isotopic compositions of chondrites and silicate planetary reservoirs, Geochim. Cosmochim. Acta 183, 14-30.

Schönbächler, M., Carlson, R.W., Horan, M.F., Mock, T.D., Hauri, E.H., 2010. Heterogeneous accretion and the moderately volatile element budget of Earth.Science. 328, 884-887.

Schuessler, J.A., Schoenberg, R., Behrens, H., von Blanckenburg, F., 2007. The experimental calibration of the iron isotope fractionation factor between pyrrhotite and peralkaline rhyolitic melt. Geochim. Cosmochim. Acta 71, 417-433.

Shahar, A., Hillgren, V.J., Horan, M.F., Mesa-Garcia, J., Kaufman, L.A., Mock, T.D., 2015. Sulfur-controlled iron isotope fractionation experiments of core formation in planetary bodies. Geochim. Cosmochim. Acta 150, 253-264.

Shahar, A., Hillgren, V.J., Young, E.D., Fei, Y.W., Macris, C.A., Deng, L.W., 2011. High-temperature Si isotope fractionation between iron metal and silicate. Geochim. Cosmochim. Acta 75, 7688-7697.

Shahar, A., Young, E.D., Manning, C.E., 2008. Equilibrium high-temperature Fe isotope fractionation between fayalite and magnetite: An experimental calibration. Earth Planet. Sci. Lett. 268, 330-338.

Shahar, A., Ziegler, K., Young, E.D., Ricolleau, A., Schauble, E.A., Fei, Y.W., 2009. Experimentally determined Si isotope fractionation between silicate and Fe metal and implications for Earth's core formation. Earth Planet. Sci. Lett. 288, 228-234.

Shahar, A. Schauble, E.A. Caracas, R., Gleason, A.E., Reagan, M.M., Xiao, Y., 2016. Pressure-dependent isotopic composition of iron alloys, Science 352, 580-582.

Siebert, J., Badro, J., Antonangeli, D., Ryerson, F.J., 2012. Metal-silicate partitioning of Ni and Co in a deep magma ocean. Earth Planet. Sci. Lett. 321, 189-197.

Siebert, J., Corgne, A., Ryerson, F.J., 2011. Systematics of metal-silicate partitioning for many siderophile elements applied to Earth's core formation. Geochim. Cosmochim. Acta 75, 1451-1489.

Siebert J., Badro, J., Antonangeli, D., Ryerson F.J., 2013. Terrestrial accretion under oxidizing conditions, Science 339, 1194-1197.

Sossi, P.A., O'Neill, H.S., 2017. The effect of bonding environment on iron isotope fractionation between minerals at high temperature. Geochim. Cosmochim. Acta 196, 121-143.

Sossi, P.A., Nebel, O., Foden, J. 2016. Iron isotope systematics in planetary reservoirs, Earth Planet. Sci. Lett., 452, 295-308.

Suer, T.-A., Siebert, J., Remusat, L., Menguy, N., Fiquet, G., 2017. A sulfur-poor terrestrial core inferred from metal–silicate partitioning experiments, Earth Planet. Sci. Lett., 469, 84-97.

Sturhahn, W., Kohn, V.G., 1999. Theoretical aspects of incoherent nuclear resonant scattering. Hyperf. Inter. 123/124, 367–399.

Sturhahn, W., 2004. Nuclear resonant spectroscopy. J. Phys. Condens. Matter. 16, S497.

Sturhahn, W., and Jackson, J.M., 2007. Geophysical application of nuclear resonant spectroscopy. Geol. Soc. Am. Spec. Pap. 421,157-174.

Teng, F.Z., Dauphas, N., Huang, S., Marty, B., 2013. Iron isotopic systematics of oceanic basalts, Geochim. Cosmochim. Acta 107, 12-26.Thibault, Y., Walter, M.J., 1995. The Influence of Pressure and Temperature on the Metal-Silicate Partition-Coefficients of Nickel and Cobalt in a Model-C1 Chondrite and Implications for Metal Segregation in a Deep Magma Ocean. Geochim. Cosmochim. Acta 59, 991-1002.

Urey H. C., 1947. The Thermodynamic Properties of Isotopic Substances. J. Chem. Soc., 562-581.

Van der Laan, S., Zhang, Y.X., Kennedy, A.K., Wyllie, P.J., 1994. Comparison of element and isotope diffusion of K and Ca in multicomponent silicate melts. Earth Planet. Sci. Lett. 123, 155-166.

van Westrenen, W., Van Orman, J.A., Watson, H., Fei, Y.W., Watson, E.B., 2003. Assessment of temperature gradients in multianvil assemblies using spinel layer growth kinetics. Geochem. Geophy. Geosy. 4, -.

Wade, J., Wood, B.J., 2005. Core formation and the oxidation state of the Earth. Earth Planet. Sci. Lett. 236, 78–95.

Wagner, C., 1952. Thermodynamics of alloys. Addison-Wesley Press, Cambridge, MA.

Wang, S., Stebbins, J.F., 1998. On the structure of borosilicate glasses: a triple-quantum magic-

angle spinning ^{17}O nuclear magnetic resonance study, J. Non-Cryst. Solids, 231, 286-290.

Watson, E.B., Wark, D.A., Price, J.D., Van Orman, J.A., 2002. Mapping the thermal structure of solid-media pressure assemblies. Contrib. Mineral. Petrol. 142, 640-652.

Weyer S., Anbar A. D., Brey G. P., Munker C., Mezger K., and Woodland A. B., 2005. Iron isotope fractionation during planetary differentiation. Earth Planet. Sci. Lett. 240, 251-264.

Willbold, M., Elliott, T., 2016. Molybdenum isotope variations in magmatic rocks. Chem. Geol. 449, 253-268.

Williams, H.M., Wood, B.J., Wade, J., Frost, D.J., Tuff, J., 2012. Isotopic evidence for internal oxidation of the Earth's mantle during accretion. Earth Planet. Sci. Lett. 231-322, 54-63.

Williams, H. M., Markowski ,A., Quitte, G., Halliday, A.N., Teutsch, N., Levasseur, S., 2006. Fe isotope fractionation in iron meteorites: New insights into metal-sulphide segregation and planetary accretion. Earth Planet. Sci. Lett. 250, 486-500.

Wood B.J., Li J., Shahar A. 2013. Carbon in the core: its influence on the properties of core and mantle, in Rev. Min. Geochem.75, 231-250.

Wood, B.J., Kiseeva, E.S., Mirolo, F.J., 2014. Accretion and core formation: the effects of sulfur on metal–silicate partition coefficients, Geochim. Cosmochim. Acta 145, 248-267.

Young, E.D., Tonui, E., Manning, C.E., Schauble, E., Macris, C.A., 2009. Spinel–olivine magnesium isotope thermometry in the mantle and implications for the Mg isotopic composition of Earth, Earth Planet. Sci. Lett. 288, 524-533

Young, E.D., Fei, Y.W., Macris, C.A., Deng, L.W., 2011. High-temperature Si isotope fractionation between iron metal and silicate. Geochim. Cosmochim. Acta 75, 7688-7697.

Young, E.D., Manning, C.E., Schauble, E.A. Shahar, A., Macris, C.A., Lazar, C., Jordan M., 2015. High-temperature equilibrium isotope fractionation of non-traditional stable isotopes: Experiments, theory, and applications, Chemical Geology 395, 176-195

Yu, G., Jacobsen, S.B., 2012. Core formation memory of siderophile elements in Earth and Mars, 43rd Lunar and Planetary Science Conference, Abstr. #1573.

Zambardi, T., Poitrasson, F., 2011. Precise determination of silicon isotopes in silicate rock reference materials by MC-ICP-MS. Geostand Geoanal Res 35, 89-99.

Zambardi, T., Poitrasson, F., Corgne, A., Méheut, M., Quitté, G., Anand, M., 2013. Silicon isotope variations in the inner solar system: Implications for planetary formation, differentiation and composition. Geochim. Cosmochim. Acta 121, 67-83.

Ziegler, K., Young, E.D., Schauble, E.A., Wasson, J.T., 2010. Metal-silicate silicon isotope fractionation in enstatite meteorites and constraints on Earth's core formation. Earth Planet. Sci. Lett. 295, 487-496.

Zou, G.T., Ma, Y.Z., Mao, H.K., Hemley, R.J., Gramsch, S.A., 2001. A diamond gasket for the laser-heated diamond anvil cell. Rev Sci Instrum 72, 1298-1301.

Figure captions:

Figure 1. Comparison of Fe isotope fractionation factor between metal and olivine calculated using the empirical method (blue line, see text) and nuclear spectroscopy measurements using the NRIXS method (red line). The empirical estimate of the β-factor for metal was calculated using the Debye temperature of pure iron while the β-factor for silicate was estimated using the approach described in Young et al. (2015).

Figure 2. Schematic diagram illustrating the trajectories of Si isotope compositions for the metal and silicate during a high temperature experiment. The yellow line indicates the mass fractionation line. The starting composition of the metal and silicate are marked with a dark red and green squares respectively. The final compositions of metal and silicate are offset by a value corresponding to the isotope fractionation factor Δ^{30}Si.

Figure 3. Three-isotope diagrams illustrating the trajectories of metal and silicate isotope composition using a standard isotope equilibration model for Si isotopes (see text for details). (a) Si isotope trajectoires for metal and silicate for variable values of the timescale of chemical equilibration (τ=600 (curve a), 1200 (curve b) 1800 minutes, (curve c)). The initial fraction of Si in the metal is assumed to be 0.1 (f_{met}^0) while the equilibrium value is 0.5. (b) Si isotope trajectories for metal and silicates assuming constant time scale and variable final values of the fraction of Si in the metal (0.1, 0.2, 0.3 and 0.4), as labeled on the curves. The initial fraction of Si in the metal is assumed to be 0.1. A straight line is obtained for $f_{eq}=f_{met}^0$. Other parameters: k_f=0.01 min^{-1}, α_{met_sil}=0.9997 for the ^{29}Si/^{28}Si ratio.

Figure 4. Three-isotope diagram illustrating the trajectories of metal and silicate Fe isotope composition using a diffusive equilibration model (see text for details). The trajectories of the metal (red line) and silicate (blue line) are quasi-linear in this diagram in the context of a diffusive model with a β value equal to 0.2. A non-linear trajectory is observed when β=5 which is unrealistically high. See text for details. The slope of the metal and silicate pair should be equal to 3/2 in this diagram.

Figure 5. Compilation of silicon isotope data (δ^{30}Si relative to the NBS 28 standard) for the bulk silicate Earth (blue squares) and chondrites from the literature (req squares). The data is

shown with 2SD error bars. There is a clear distinction between the bulk silicate Earth and chondrites (ordinary or carbonaceous), except for the data set of Chakrabarti and Jacobsen (2010). Data from Georg et al. 2007; Fitoussi et al. 2009; Savage et al. 2010; Chakrabarti and Jacobsen 2010; Armytage et al. 2011; Savage and Moynier 2013; Zambardi et al. 2013.

Figure 6. Compilation of chromium isotope data ($\delta^{53}Cr$) for the bulk silicate Earth (blue squares) and chondrites (req squares) from the literature. The data is shown with 2SD error bars. There is no difference between the BSE and chondrites, except for the data set of Moynier et al. (2011).

Figure 5. Iron isotope fractionation factors between liquid metal and liquid silicate at 1650°C against atomic fraction of sulphur in the liquid metal. Unless otherwise indicated, experiments were performed at 1 GPa and only contained metallic Fe, Ni and S in the metallic form in the starting mixture. Hin=Hin et al. (2012), S-free experiment in graphite capsule, S-bearing experiment in SiO_2 glass capsule; Poitrasson=Poitrasson et al. (2009), all experiments in graphite capsules; Shahar=Shahar et al. (2015), all experiments in BN capsules. Liu=Liu et al. (2017), based on NRIXS data (in diamond anvil cell) for Fe_3S and basaltic glass.

Figure 8 Compilation of molybdenum isotope data ($\delta^{98}Mo$) for the bulk silicate Earth (blue squares) and chondrites (req squares) from the literature. The data is shown with 2SD error bars.

Figure 9 (a) Model calculations of the Si metal-silicate partition coefficient during accretion. The mean value of Si metal-silicate partition coefficient is approximately 0.3 for the Earth, which corresponds to f_{O2} conditions ranging between IW-3.5 and IW-3.7 (starting composition, depending on the Earth's core composition 3 to 7 wt%). (b) Model calculations for the difference between the $\delta^{30}Si$ of the bulk silicate Earth and the $\delta^{30}Si$ of the bulk Earth using the model described in section 5 for variable starting f_{O2} values relative to the IW buffer, as labelled on the curves. The model uses a variable f_{O2} throughout accretion and assumes that the mass fraction of equilibrated core material (k) is 0.5. The final f_{O2} of the accreted material is 1.5 log units higher than the starting value and the evolution of f_{O2} follows equation (33). The vertical arrow indicates the range of values of $\Delta^{30}Si_{BSE\_BE}$ from the literature as compiled in Hin et al.

(2014). The oxygen fugacity in the embryos is IW-3.5 and the pressure of metal silicate equilibration is 5 GPa for a temperature of 2115 K.

Figure 10. (a) Model calculations of the Cr metal-silicate partition coefficient during accretion. The mean value of Cr metal-silicate partition coefficient is approximately 3.5 for the Earth, which corresponds to f_{O2}conditions between IW-3 and IW-3.5 (starting composition). (b) Model calculations for the difference between the δ^{52}Cr of the bulk silicate Earth and the δ^{52}Cr of the bulk Earth using the model described in section 5 for variable starting f_{O2}values relative to the IW buffer, as labelled on the curves. The model uses a variable f_{O2} throughout accretion and assumes that the mass fraction of equilibrated core material (k) is 0.5. The final f_{O2} of the accreted material is 1.5 log units higher than the starting value and the evolution of f_{O2} follows equation (33). Based on existing uncertainties, the maximum value of measured $\Delta^{53}Cr_{BSE\_BE}$ is well above (>0.1‰) the final value calculated in the models (Bonnand et al. 2016; Schoenberg et al. 2016, Qin et al. 2015). The oxygen fugacity in the embryos is IW-3.5 and the pressure of metal silicate equilibration is 5 GPa for a temperature of 2115 K.

Figure 11. (a) Model calculations of the Mo metal-silicate partition coefficient during accretion. (b) Model calculations for the difference between the δ^{98}Mo of the bulk silicate Earth and the δ^{98}Mo of the bulk Earth using the model described in section 5 for variable starting f_{O2} values relative to the IW buffer, as labelled on the curves. The model uses a variable f_{O2}throughout accretion and assumes that the mass fraction of equilibrated core material (k) is 0.5. The final f_{O2} of the accreted material is 1.5 log units higher than the starting value and the evolution of f_{O2} follows equation (33). Based on existing uncertainties, the maximum value of observed $\Delta^{95}Mo_{BSE\_BE}$ is not greater than 0.1‰ and could be as low as 0‰, which is consistent with the models. The oxygen fugacity in the embryos is IW-3.5 and the pressure of metal silicate equilibration is 5 GPa for a temperature of 2115 K.

Figure 12. Model curves illustrating the effect of the degree of metal-silicate equilibration for various values of the parameter k, as labeled on the curves. The starting value of the f_{O2}relative to IW is -3.5 while the final value is -2. The corresponding metal-silicate partition coefficient is shown in Figure 9. The oxygen fugacity in embryos is IW-3.5 and the pressure of metal silicate equilibration is 5 GPa for a temperature of 2115 K. The greatest fractionation is observed for the largest value of k, as there is a strong dependence of the metal-silicate

partition coefficient to T and P, which means that the terrestrial conditions are better to produce fractionation relative to the embryos. Vertical double arrow corresponds to the observed range.

Figure 13. Model curves for illustrating the effect of partial equilibration using the parameterization of Deguen et al. (2014) for various values of the parameter Δm (see text for details), as labeled on the curves. All other parameters are identical to the conditions in Figure 9 with a starting f_{O2}=IW-3.5 and k=0.5. The largest Si isotope fractionation is obtained for large values of Δm, corresponding to more efficient equilibration of metal and silicate. The oxygen fugacity in the embryos is IW-3.5 and the pressure of metal silicate equilibration is 5 GPa for a temperature of 2115 K.

1728

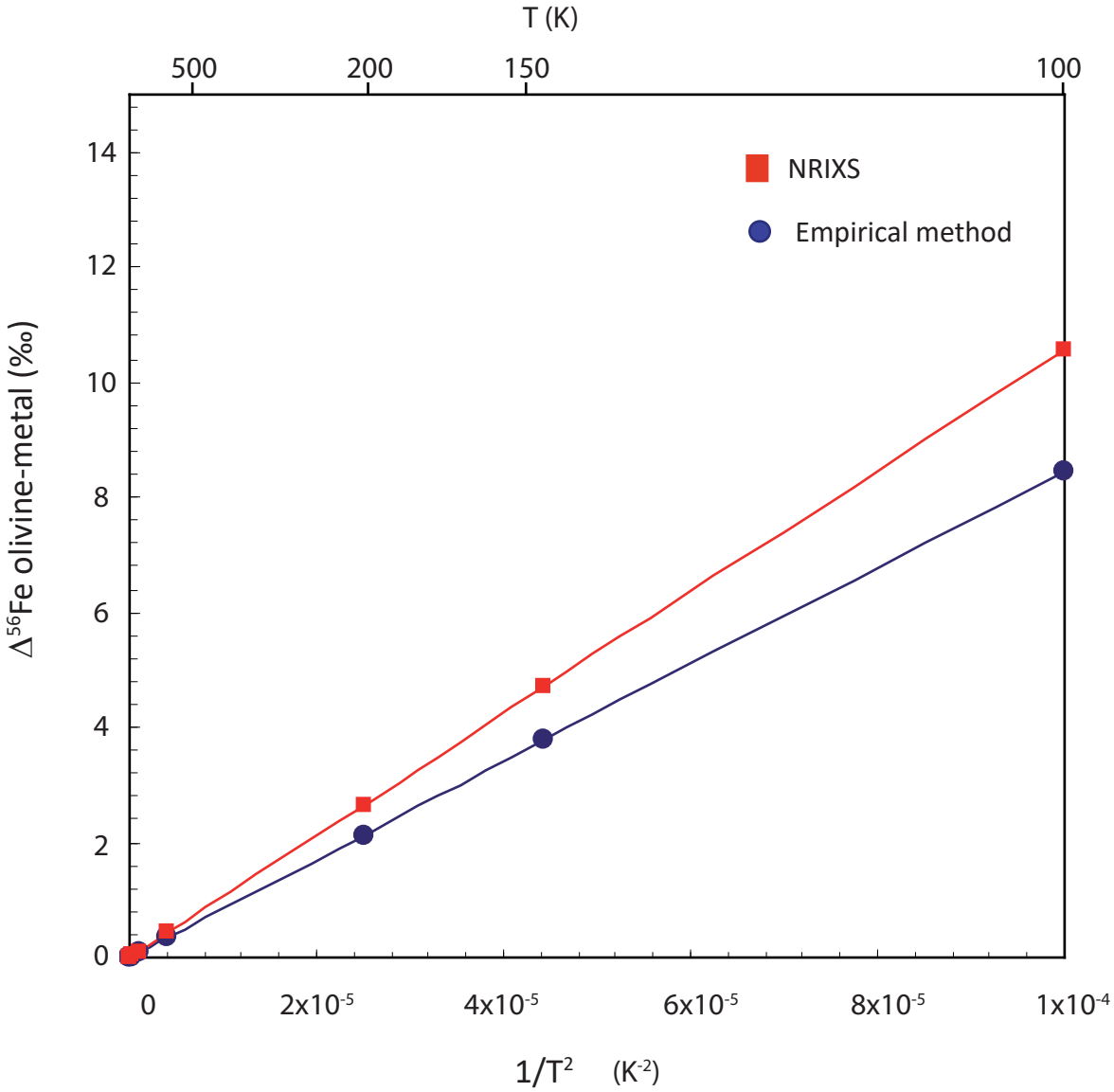
T (K)
500
200
150
100
14
12
10
8
6
4
2
0
NRIXS
Empirical method
Δ^{56}Fe olivine-metal (‰)
0
2x10^{-5}
4x10^{-5}
6x10^{-5}
8x10^{-5}
1x10^{-4}
1/T^2 (K^{-2})

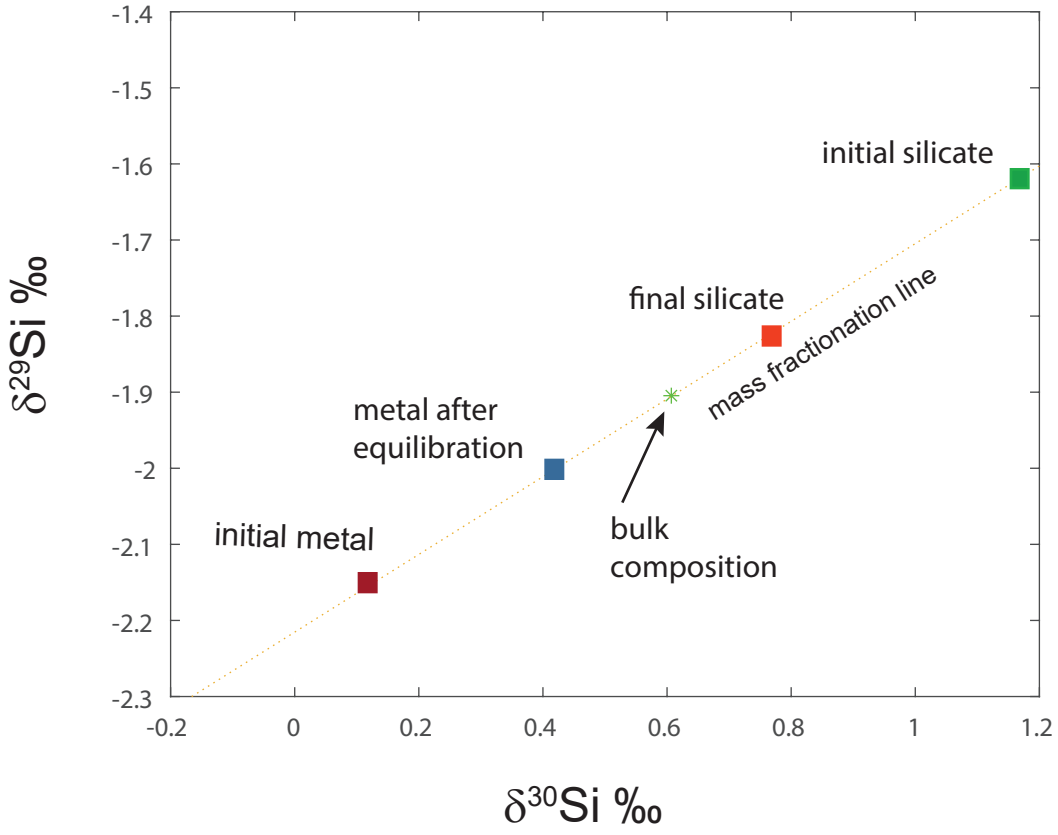
-1.4
-1.5
-1.6
-1.7
-1.8
-1.9
-2
-2.1
-2.2
-2.3
-0.2
0
0.2
0.4
0.6
0.8
1
1.2
δ29Si ‰
δ30Si ‰
initial silicate
final silicate
mass fractionation line
metal after
equilibration
initial metal
bulk
composition

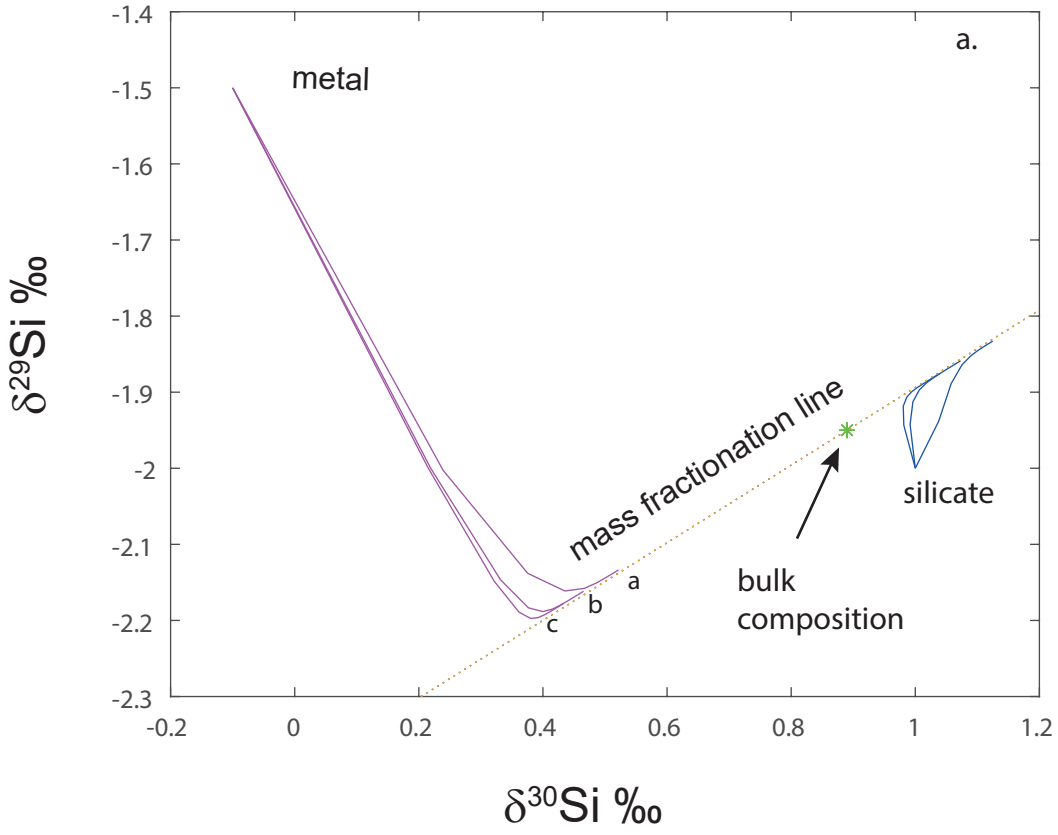
a.
metal
mass fractionation line
silicate
bulk
composition
a
b
c
-1.4
-1.5
-1.6
-1.7
-1.8
-1.9
-2
-2.1
-2.2
-2.3
-0.2
0
0.2
0.4
0.6
0.8
1
1.2
δ29Si ‰
δ30Si ‰

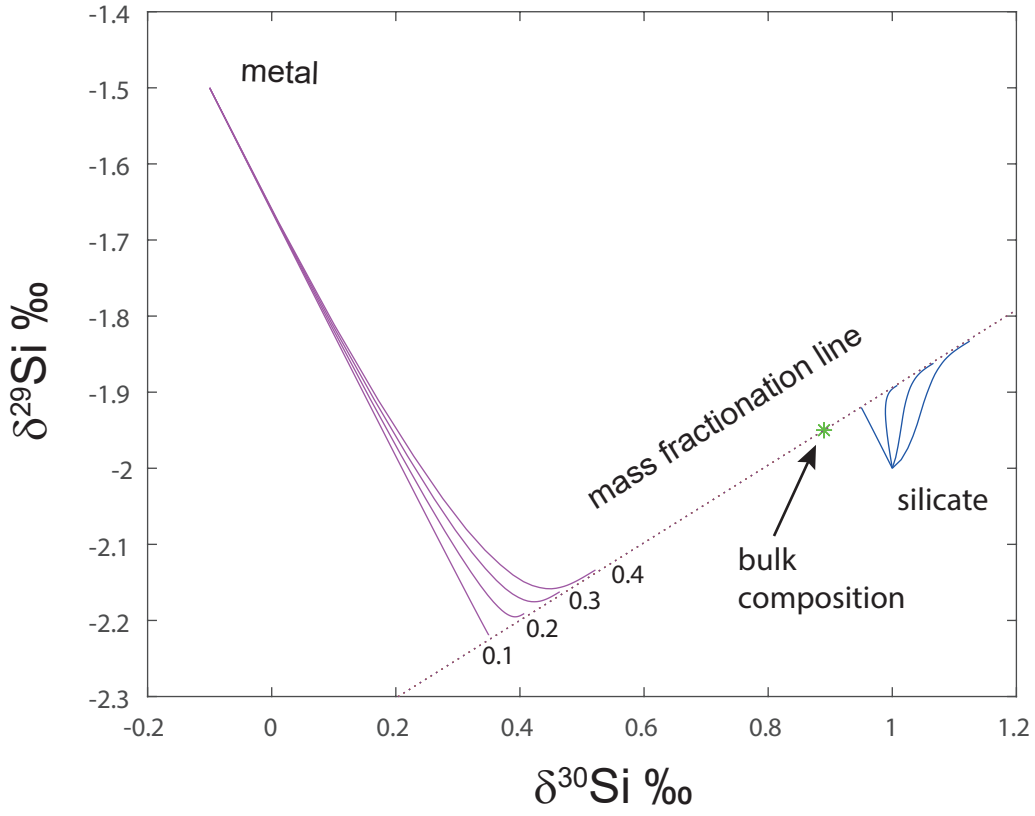
metal
mass fractionation line
silicate
bulk
composition
0.1
0.2
0.3
0.4
-1.4
-1.5
-1.6
-1.7
-1.8
-1.9
-2
-2.1
-2.2
-2.3
-0.2
0
0.2
0.4
0.6
0.8
1
1.2
δ29Si ‰
δ30Si ‰

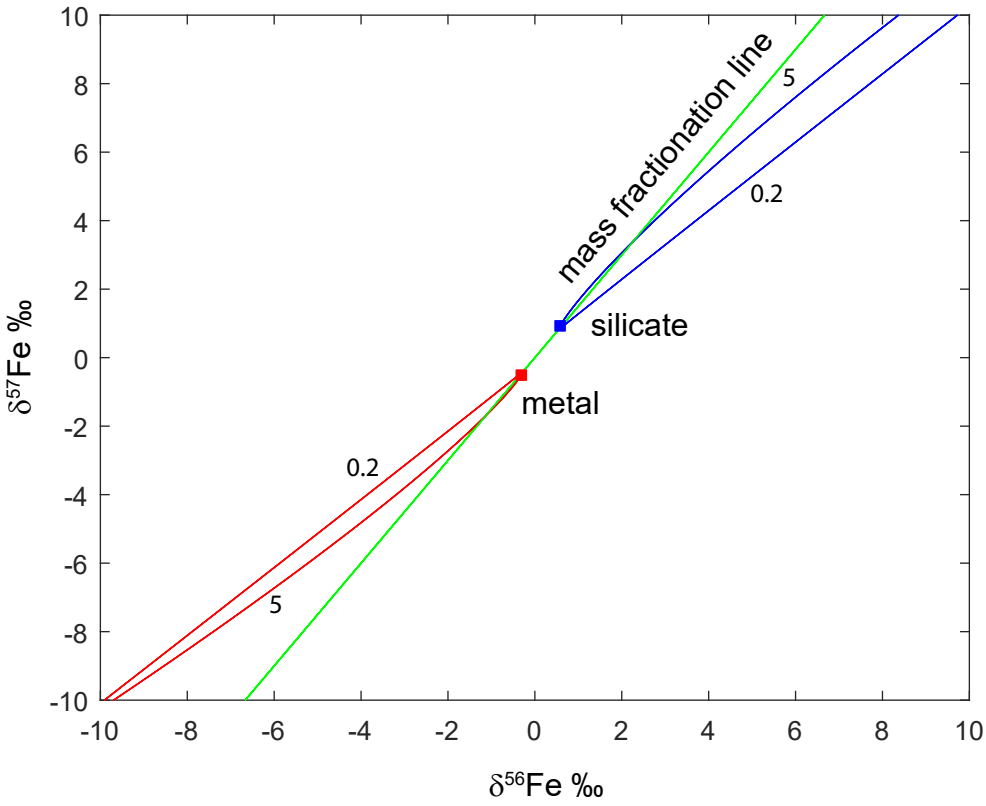
mass fractionation line
5
0.2
silicate
metal
0.2
5
δ57Fe ‰
δ56Fe ‰
10
8
6
4
2
0
-2
-4
-6
-8
-10
-10
-8
-6
-4
-2
0
2
4
6
8
10

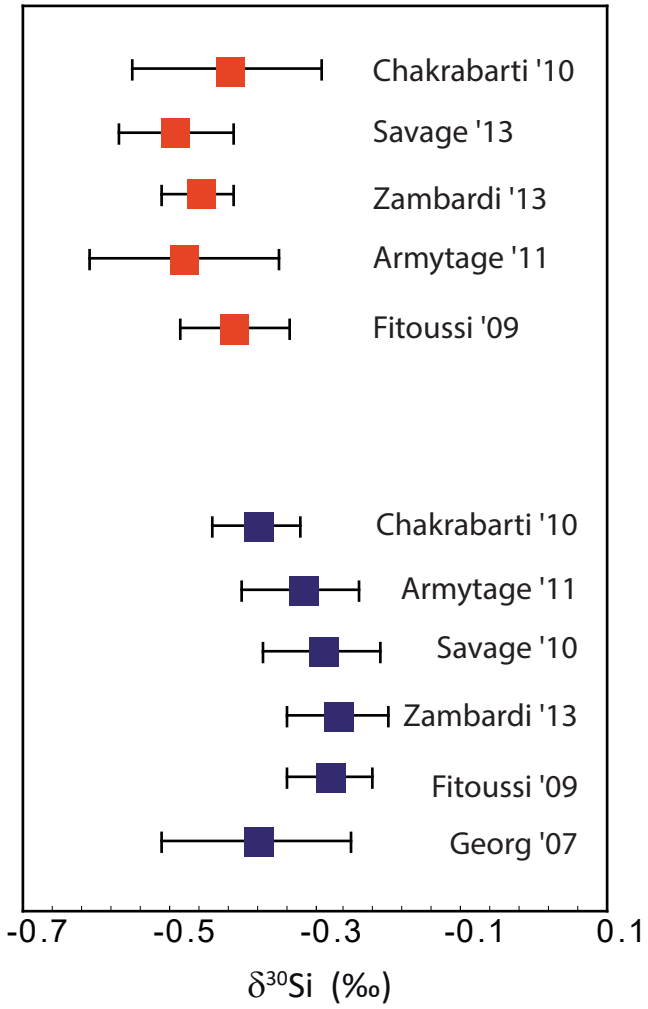
Chakrabarti '10
Savage '13
Zambardi '13
Armytage '11
Fitoussi '09
Chakrabarti '10
Armytage '11
Savage '10
Zambardi '13
Fitoussi '09
Georg '07
-0.7
-0.5
-0.3
-0.1
0.1
δ30Si (‰)

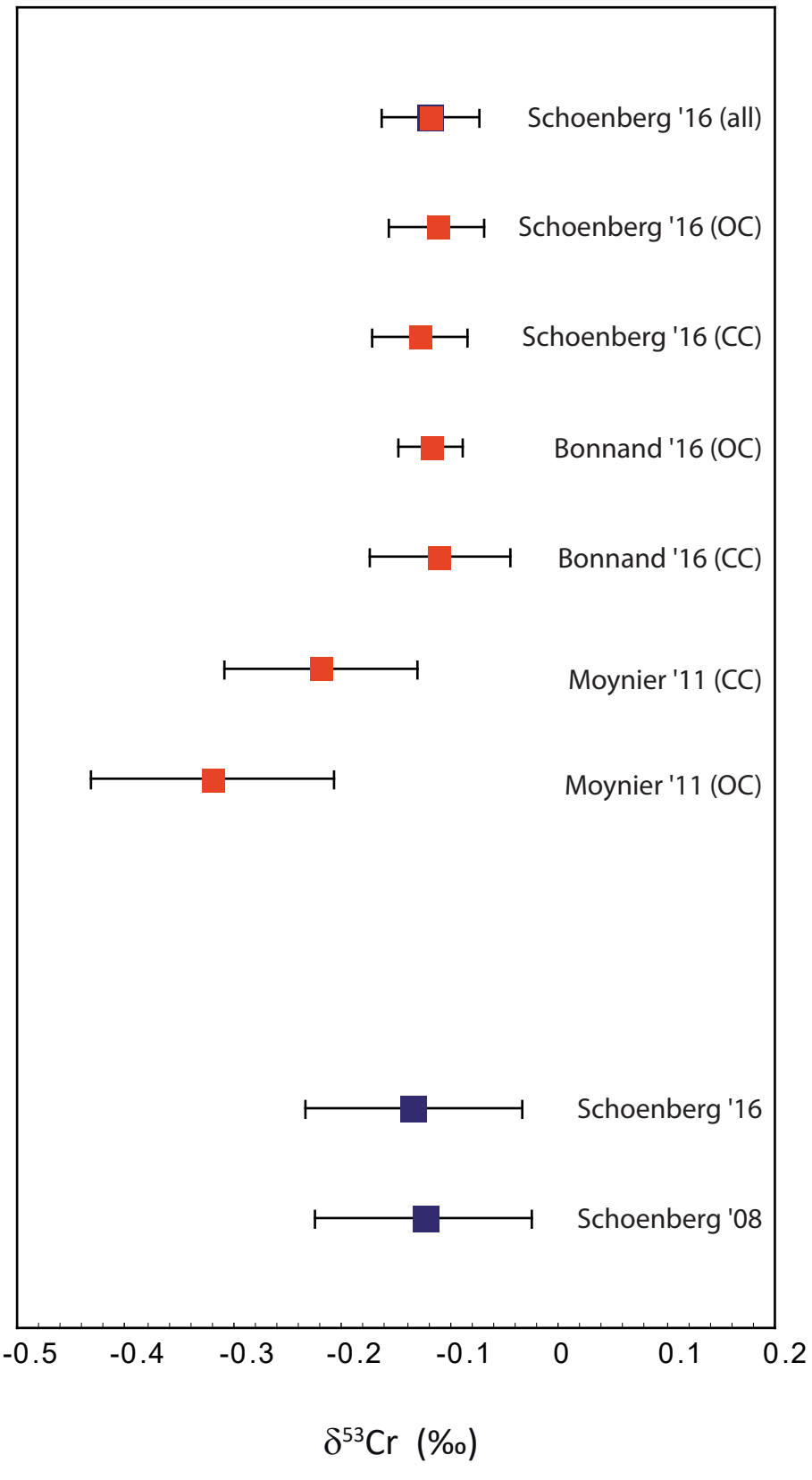
Schoenberg '16 (all)
Schoenberg '16 (OC)
Schoenberg '16 (CC)
Bonnand '16 (OC)
Bonnand '16 (CC)
Moynier '11 (CC)
Moynier '11 (OC)
Schoenberg '16
Schoenberg '08
-0.5
-0.4
-0.3
-0.2
-0.1
0
0.1
0.2
δ53Cr (‰)

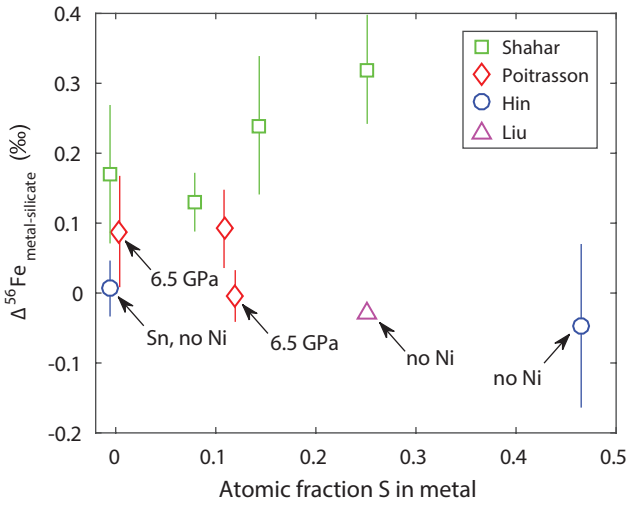

Figure 2. Iron isotope fractionation factors between liquid metal and liquid silicate against atomic fraction of sulphur in the metal liquid. Unless otherwise indicated, experiments were performed at 1 GPa and only contained metallic Fe, Ni and S in metallic form in the starting mixture. Hin = Hin et al. (2012), S-free experiment in graphite capsule, S-bearing experiment in SiO_2 glass capsule; Poitrasson = Poitrasson et al. (2009), all experiments in graphite capsules; Shahar = Shahar et al. (2015), all experiments in BN capsules.

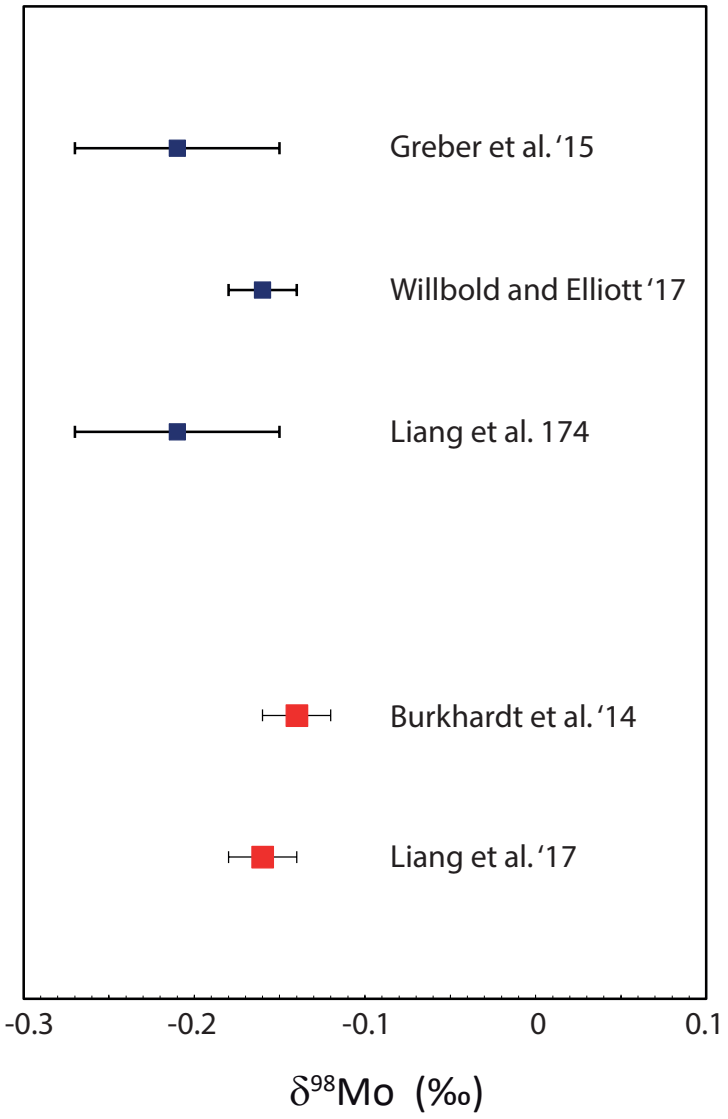
Greber et al. '15
Willbold and Elliott '17
Liang et al. 174
Burkhardt et al. '14
Liang et al. '17
-0.3
-0.2
-0.1
0
0.1
δ98Mo (‰)

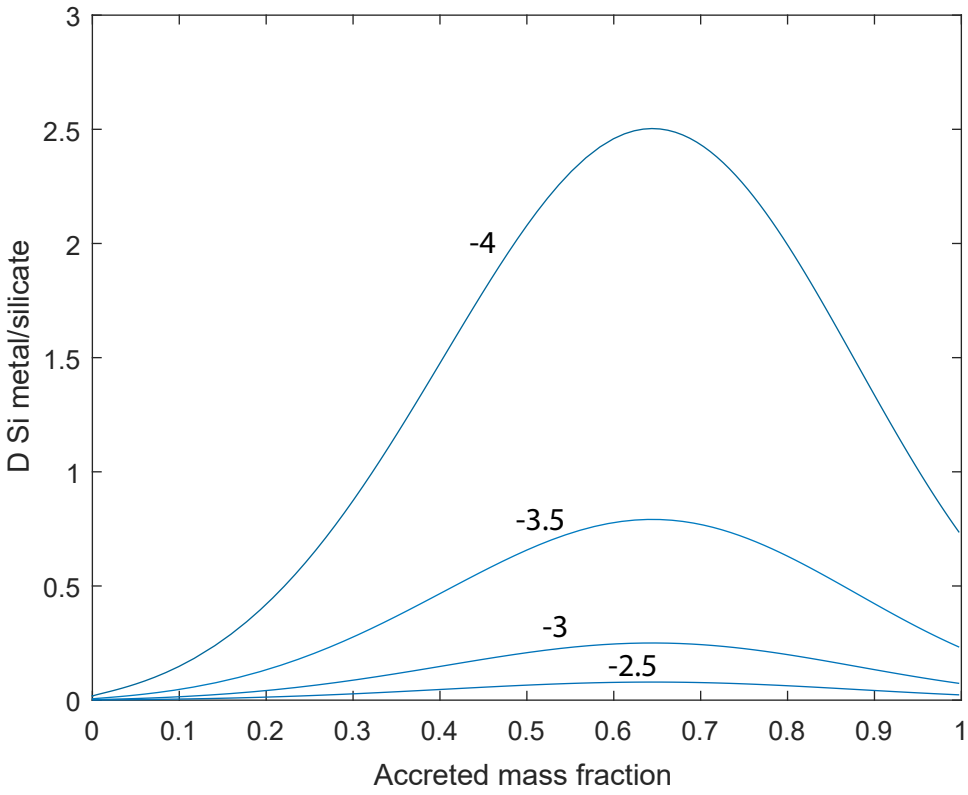
D Si metal/silicate
Accreted mass fraction
-4
-3.5
-3
-2.5
0
0.5
1
1.5
2
2.5
3
0
0.1
0.2
0.3
0.4
0.5
0.6
0.7
0.8
0.9
1

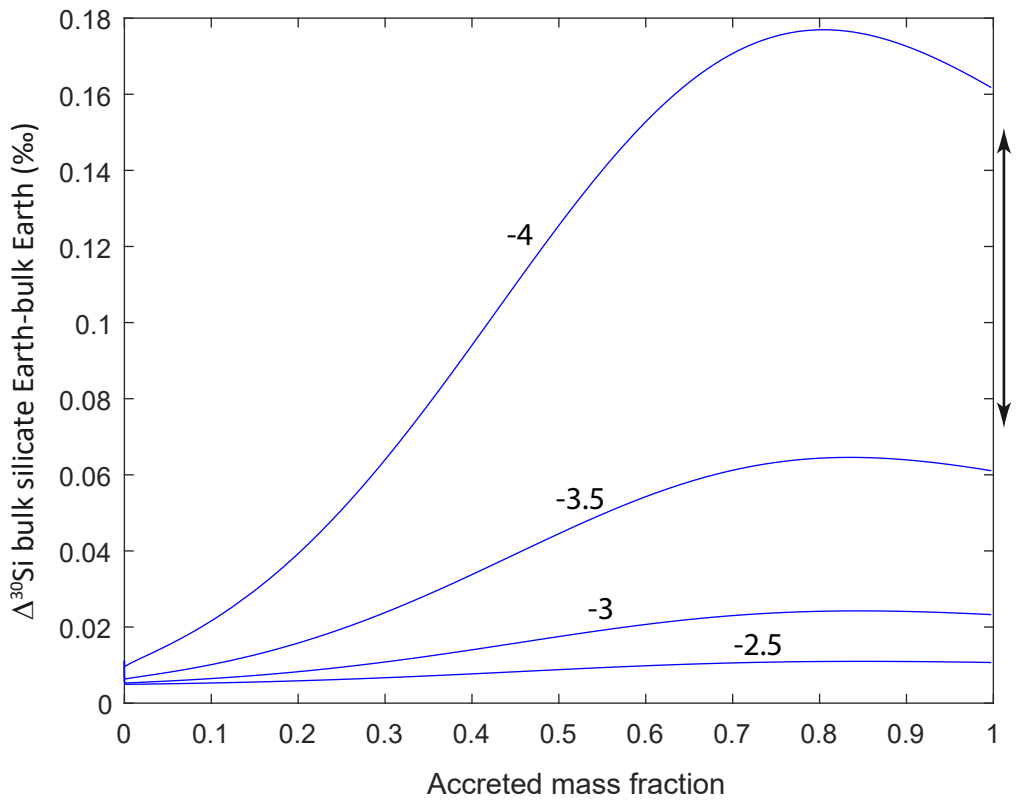
0.18
0.16
0.14
0.12
0.1
0.08
0.06
0.04
0.02
0
0
0.1
0.2
0.3
0.4
0.5
0.6
0.7
0.8
0.9
1
Δ30Si bulk silicate Earth-bulk Earth (‰)
Accreted mass fraction
-4
-3.5
-3
-2.5

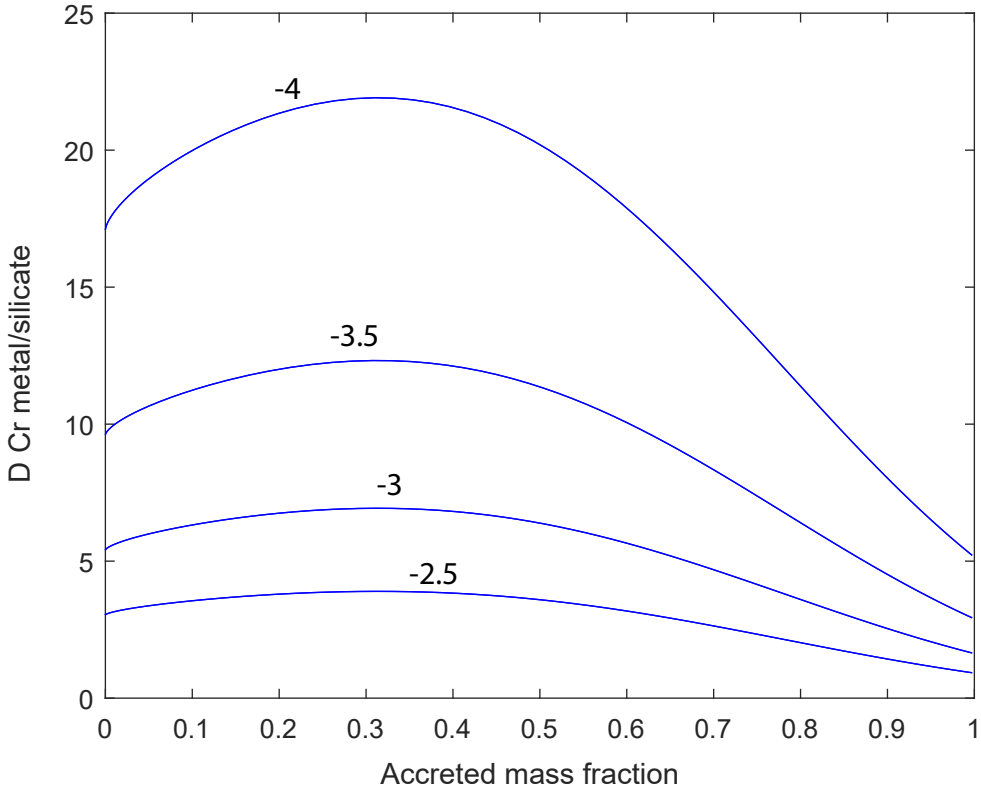
25
20
15
10
5
0
0
0.1
0.2
0.3
0.4
0.5
0.6
0.7
0.8
0.9
1
D Cr metal/silicate
Accreted mass fraction
-4
-3.5
-3
-2.5

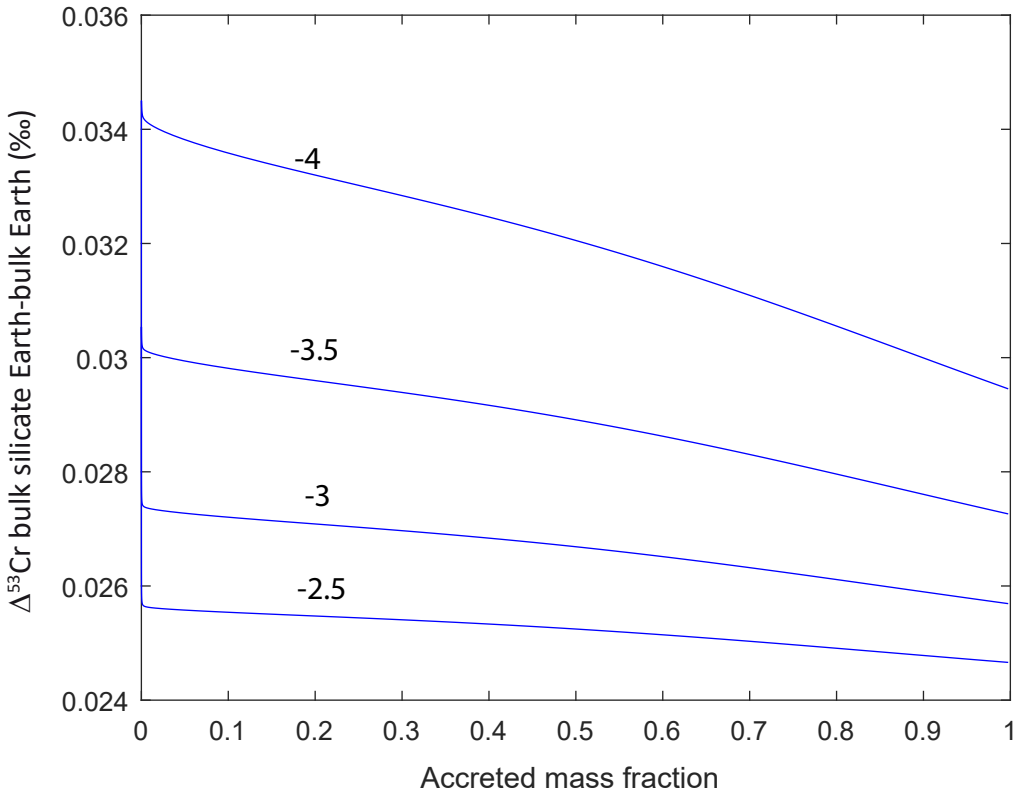
0.036
0.034
0.032
0.03
0.028
0.026
0.024
0
0.1
0.2
0.3
0.4
0.5
0.6
0.7
0.8
0.9
1
Accreted mass fraction
Δ53Cr bulk silicate Earth-bulk Earth (‰)
-4
-3.5
-3
-2.5

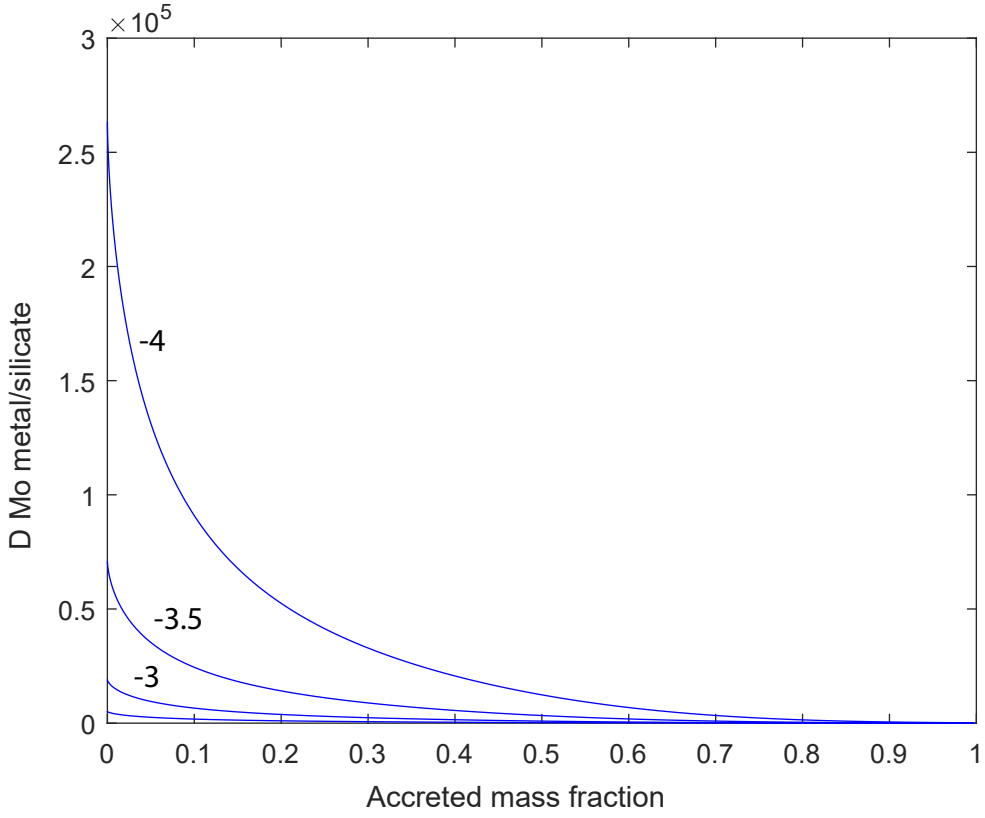
×10^5
3
2.5
2
1.5
1
0.5
0
D Mo metal/silicate
-4
-3.5
-3
0
0.1
0.2
0.3
0.4
0.5
0.6
0.7
0.8
0.9
1
Accreted mass fraction

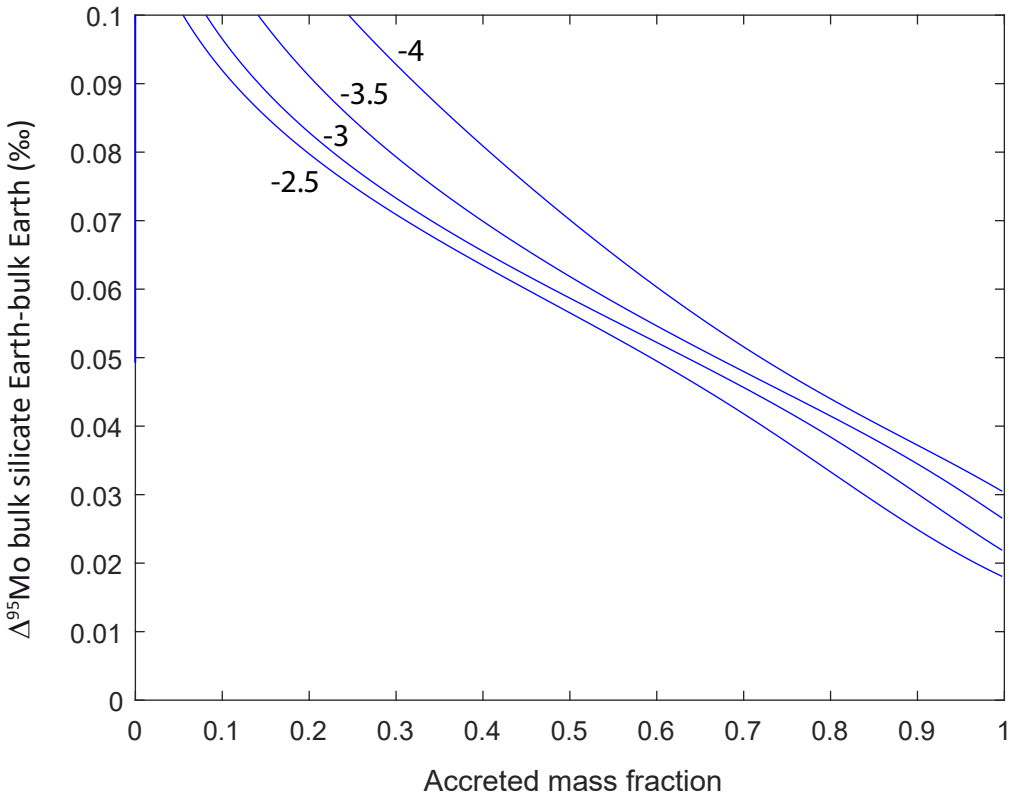
0.1
0.09
0.08
0.07
0.06
0.05
0.04
0.03
0.02
0.01
0
0
0.1
0.2
0.3
0.4
0.5
0.6
0.7
0.8
0.9
1
-4
-3.5
-3
-2.5
Δ95Mo bulk silicate Earth-bulk Earth (‰)
Accreted mass fraction

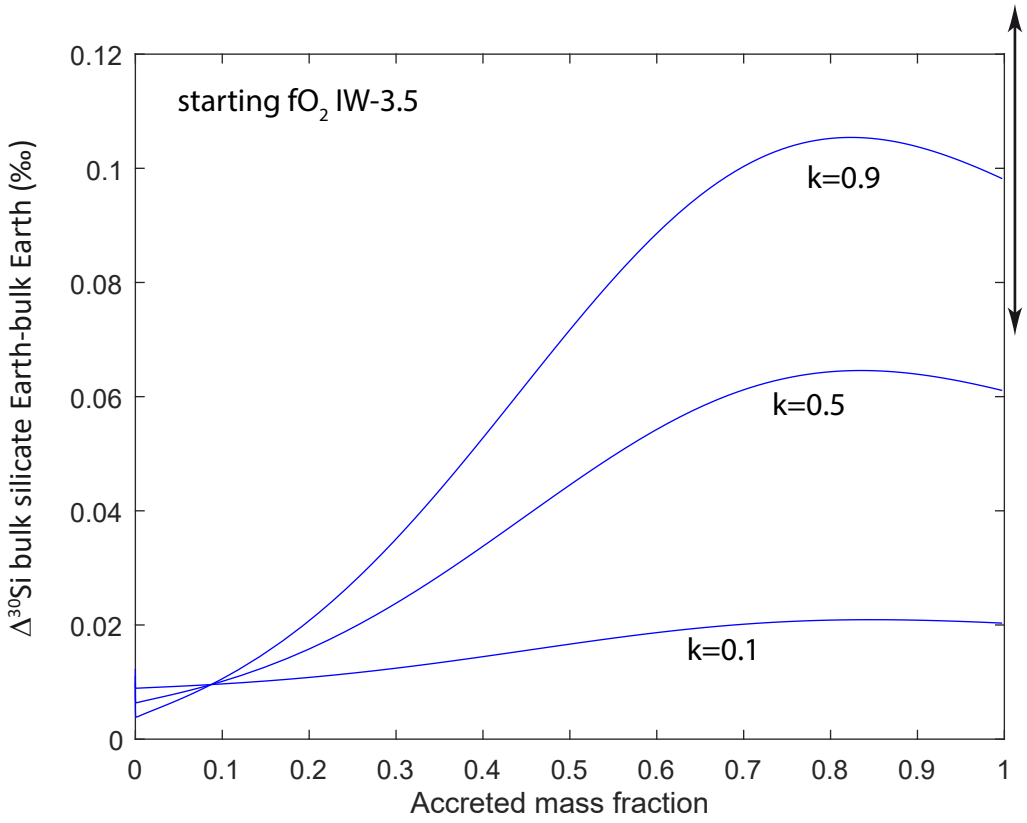
starting fO2 IW-3.5
k=0.9
k=0.5
k=0.1
Δ30Si bulk silicate Earth-bulk Earth (‰)
Accreted mass fraction
0.12
0.1
0.08
0.06
0.04
0.02
0
0
0.1
0.2
0.3
0.4
0.5
0.6
0.7
0.8
0.9
1

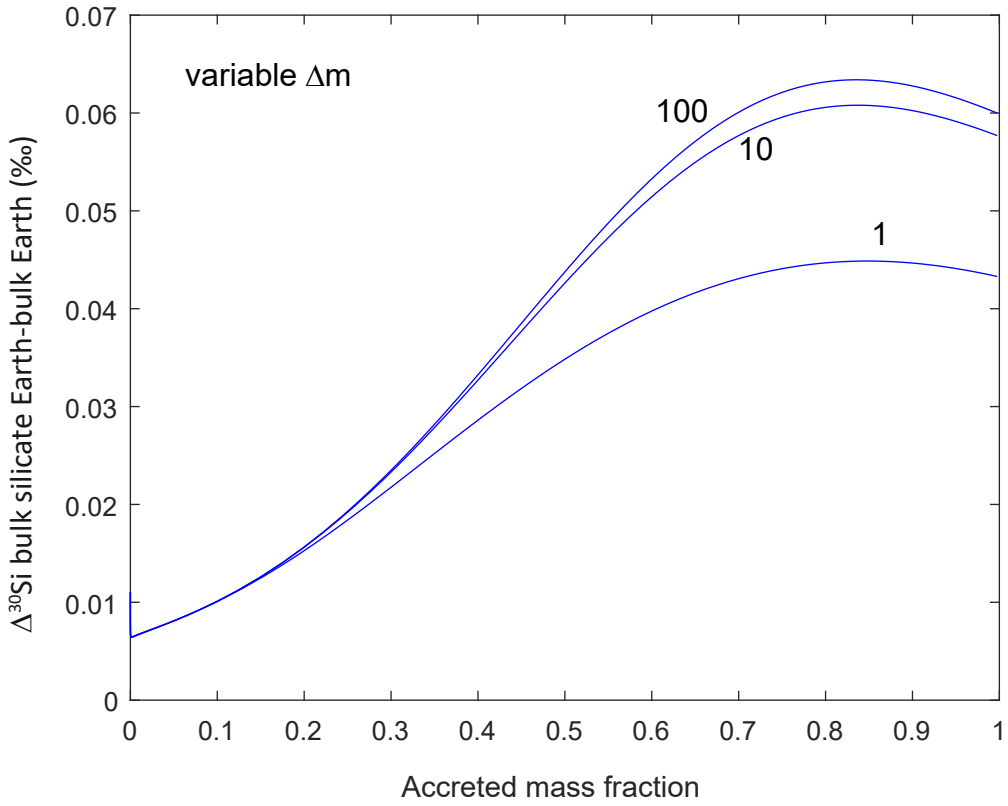
variable Δm
100
10
1
0.07
0.06
0.05
0.04
0.03
0.02
0.01
0
0
0.1
0.2
0.3
0.4
0.5
0.6
0.7
0.8
0.9
1
Δ30Si bulk silicate Earth-bulk Earth (‰)
Accreted mass fraction